Identification and quantification of phosphatidylcholines containing very-long-chain polyunsaturated fatty acid in bovine and human retina using liquid chromatography/tandem mass spectrometry

Olivier Berdeaux, Pierre Juaneda, Lucy Martine, Stéphanie Cabaret, Lionel Brétillon, Niyazi Acar

▶ To cite this version:

HAL Id: hal-01137063

https://hal.science/hal-01137063

Submitted on 30 Mar 2015

Accepted Manuscript

Title: Identification and quantification of phosphatidylcholines containing very-long-chain polyunsaturated fatty acid in bovine and human retina using liquid chromatography/tandem mass spectrometry

Authors: Olivier Berdeaux, Pierre Juaneda, Lucy Martine, Stephanie Cabaret, Lionel Bretillon, Niyazi Acar

Please cite this article as: O. Berdeaux, P. Juaneda, L. Martine, S. Cabaret, L. Bretillon, N. Acar, Identification and quantification of phosphatidylcholines containing very-long-chain polyunsaturated fatty acid in bovine and human retina using liquid chromatography/tandem mass spectrometry, *Journal of Chromatography A* (2008), doi:10.1016/j.chroma.2010.10.039

1 **Identification and quantification of phosphatidylcholines containing very-long-chain**
2 **polyunsaturated fatty acid in bovine and human retina using liquid chromatography/tandem**
3 **mass spectrometry.**

4 Olivier Berdeaux[1*], Pierre Juaneda[2], Lucy Martine[2], Stephanie Cabaret[1], Lionel Bretillon[2] and Niyazi Acar[2]

5

6 [1] Lipid-Aroma Platform, Centre des Sciences du Goût et de l'Alimentation, UMR6265 CNRS, UMR1324 INRA,
7 Université de Bourgogne, Agrosup Dijon, F-21000 Dijon.
8
9 [2] Eye and Nutrition Research Group, Centre des Sciences du Goût et de l'Alimentation, UMR6265 CNRS,
10 UMR1324 INRA, Université de Bourgogne, Agrosup Dijon, F-21000 Dijon.

11

12 **Address for Correspondence:**

13 Olivier Berdeaux, PhD

14 Centre des Sciences du Goût et de l'Alimentation,

15 Plate-Forme "Lipides-Arômes",

16 17, rue Sully, BP86510

17 21065 Dijon Cedex

18 France

19 Fax +33-(0)3.80.69.32.23

20 Tel. +33-(0)3.80.69.35.40

21 E-mail: berdeaux@dijon.inra.fr

22

1

Abstract

The retina is one of the vertebrate tissues with the highest content in polyunsaturated fatty acids (PUFA). A large proportion of retinal phospholipids, especially those found in photoreceptor membranes, are dipolyunsaturated molecular species. Among them, dipolyunsaturated phosphatidylcholine (PC) molecular species are known to contain very-long-chain polyunsaturated fatty acids (VLC-PUFA) from the n-3 and n-6 series having 24-36 carbon atoms (C24-C36) and four to six double bonds. Recent interest in the role played by VLC-PUFA arose from the findings that a protein called Elongation of very-long-chain fatty acids 4 (ELOVL4) is involved in their biosynthesis and that mutations in the *ELOVL4* gene are associated with Stargardt-like macular dystrophy (STD3), a dominantly inherited juvenile macular degeneration leading to vision loss. The aim of the present study was to develop an HPLC-ESI-MS/MS method for the structural characterisation and the quantification of dipolyunsaturated PC molecular species containing VLC-PUFA and validate this methodology on retinas from bovines and human donors. Successful separation of phosphatidylethanolamine (PE), phosphatidylinositol (PI), phosphatidylserine (PS), PC, lyso-phosphatidylcholine (LPC) and sphingomyelin (SM) was achieved using a silica gel column and a gradient of hexane/isopropanol/water containing ammonium formate as a mobile phase. A complete structural characterisation of intact phosphatidylcholine species was obtained by collision-induced dissociation (CID) in the negative mode. Fatty acid composition and distribution can be clearly assigned based on the intensity of *sn*-2/*sn*-1 fragment ions. The PC species were characterised on bovine retina, 28 of which were dipolyunsaturated PC species containing one VLC-PUFA (C24–C36) with three to six double bonds. VLC-PUFA was always in the *sn*-1 position whilst PUFA at the *sn*-2 position was exclusively docosahexaenoic acid (DHA, C22:6n-3). Most of these VLC-PUFA-containing dipolyunsaturated PCs were detected and quantified in human retinas. The quantitative analysis of the different PC molecular species was performed in the positive mode using precursor ion scanning of *m/z* 184 and 14:0/14:0-PC and 24:0/24:0-PC as internal standards. The relationship between the MS peak intensities of different PC species and their carbon chain length was included for calibration. The main compounds represented were those having VLC-PUFA with 32 carbon atoms (C32:3, C32:4, C32:5 and C32:6) and 34 carbon atoms (C34:3, C34:4, C34:5 and C34:6). Dipolyunsaturated PCs with 36:5 and 36:6 were detected but in smaller quantities. In conclusion, this new HPLC-ESI-MS/MS method is sensitive and specific enough to structurally characterise and quantify all molecular PC species, including those esterified with VLC-PUFA. This technique is valuable for a precise characterisation of PC molecular species containing VLC-PUFA in retina and may be useful for a better understanding of the pathogenesis of STD3.

1. Introduction

The retina is one of the vertebrate tissues with the highest content of polyunsaturated fatty acids (PUFA). A large proportion of the retinal glycerophospholipids, especially those of photoreceptor membranes, consist of dipolyunsaturated molecular species. Studies have reported that dipolyunsaturated phosphatidylcholine (PC) molecular species present in both rod- and cone-dominant retinas contain 22:6n-3 as one of the acyl chains, the other one being very-long-chain (C24–C36) polyunsaturated fatty acids (four, five or six double bonds) [1-3]. The majority of these PC species containing VLC-PUFA (VLC-PC) are localised in photoreceptor outer segments where the phototransduction reactions take place [4]. In bovine photoreceptor outer segments, VLC-PC species are significant components of lipid membranes since the C28-C36 VLC-PUFA represent 10 mol % of total fatty acids in PCs [1].

Recently, at least three different mutations in a gene called *elongation of very long chain fatty acids 4* (*ELOVL4*) have been identified in patients with Stargardt-like macular dystrophy type 3 (STD3), a dominantly inherited form of juvenile macular degeneration leading to vision loss [5-8] Based on sequence homology with ELOVL1, 2, 3, and 5 proteins, which are implicated in the elongation of saturated, monounsaturated, or polyunsaturated fatty acids (PUFA) from 18 to 26 carbons, the ELOVL4 protein was predicted to have similar functions [5,8-11]. These findings suggested that retinal health depends on the presence of C28-C36 PUFA in addition to that of docosahexaenoic acid (DHA, C22:6n-3) [12].

Concurrently with these biochemical and molecular studies, a transgenic mouse model of STD3 carrying the human pathogenic 5-bp deletion in the mouse *ELOVL4* gene was developed [13]. The animals displayed a retinal phenotype resembling that of human STD3, including an early selective deficiency in retinal C28–C36 acyl PCs, followed by a reduced electroretinographic response, an increased accumulation of toxic *N*-retinylidene-*N*-retinylethanolamine (A2E) and a degeneration of photoreceptor cells in the central retina. According to these findings, the proposed pathogenesis of human STD3 is based on the alteration of rod outer segments (ROS, corresponding to the distal part of retinal photoreceptor cells) composition in VLC-PUFA affecting phototransduction and leading to the accumulation of toxic A2E and further to photoreceptor death [14].

In order to confirm this hypothesis, dipolyunsaturated PC molecular species containing VLC-PUFA in retina must be precisely characterised to improve our understanding of the pathogenesis of STD3. Several current approaches were used for the characterisation and quantification of VLC-PUFA or VLC-PC in biological samples [1,2,4,15,16], but most of these conventional approaches are time-consuming, requiring successive extraction, chromatographic steps (HPLC, TLC) and often a derivatisation step before gas chromatography (GC) or gas chromatography-mass spectrometry (GC-MS) analyses. Electrospray ionisation-mass spectrometry (ESI-MS) has been described as a soft ionisation technology [17]. It is the most sophisticated and easiest technique for assessing the phospholipid content of a biological sample because of its high sensitivity and unmatched specificity. It directly analyses phospholipids as intact molecules and preserves the information based on the relative position of acyl radicals on the glycerol backbone. Using standard equipment, ESI-MS has been widely used for characterisation [17-23] and quantification of phospholipids [24-38]. Different approaches have been adopted for the analysis of molecular species of phospholipids using ESI-MS

3

101 [39,40]. In some of these, crude lipid extracts were infused to the MS instrument and either direct MS
102 scans or specific precursor ion or neutral loss scans were utilised to determine the different lipid
103 species [29,34,36,39,41]. Other commonly used methods employed liquid chromatography with on-
104 line mass spectrometric detection (HPLC-ESI-MS) [18,22,23,25-28,31,33,35,42-44]. The combination
105 of high-performance liquid chromatography (HPLC) and ESI-MS reduces the ionisation suppression
106 effect of low abundance PL species compared to indirect ESI-MS alone [24,43,45]. Moreover, HPLC-
107 ESI-MS offers the advantage of a low spectral background signal [46]. However, the quantitative
108 analysis of PL is not as easy since MS signals of PL are influenced by different effects related to acyl
109 chain length, the degree of acyl chain unsaturation and concentration [28,34,36].

110 In this study, we propose to develop a normal-HPLC-ESI-MS/MS method using a triple quadrupole
111 mass spectrometer for precise characterisation and quantification of major PC species (including VLC-
112 PC and glyceroplasmenylcholine plasmalogen (PlsC) species) in total lipid extracts from bovine and
113 human retinas. During the quantification step, particular attention was paid to the influence of different
114 parameters related to PC acyl chain length and the degree of acyl chain unsaturation of the
115 concentration on the spectrometer response according to previous studies [27,34,36].

116 **2. Material and methods**

117 *2.2. Lipids and other materials*

118 All chemical reagents were purchased from Sigma-Aldrich (St Quentin Fallavier, France), chloroform
119 and methanol from SDS (Peypin, France). HPLC-grade N-hexane, chloroform and isopropanol, LC-
120 MS-grade methanol and water were all from Fisher Scientific (Illkirch, France). Commercially available
121 phospholipids were obtained from Avanti Polar Lipids Inc. (Alabaster, AL, USA): dimyristoyl-sn-
122 glycerol-3-phosphatidylcholine (PC 14:0/14:0), 1,2-dipalmitoyl-*sn*-glycero-3-phosphocholine (PC
123 16:0/16:0), 1-palmitoyl-2-oleoyl-*sn*-glycero-3-phosphocholine (PC 16:0/18:1), 1,2-distearoyl-*sn*-
124 glycero-3-phosphocholine (PC 18:0/18:0), 1-stearoyl-2-arachidonoyl-*sn*-glycero-3-phosphocholine (PC
125 18:0/20:4), 1-stearoyl-2-arachidonoyl-*sn*-glycero-3-phosphocholine (PC 18:0/20:4), 1-stearoyl-2-
126 docosahexaenoyl-*sn*-glycero-3-phosphocholine (PC 18:0/22:6), 1,2-diarachidoyl-*sn*-glycero-3-
127 phosphocholine (PC 20:0/20:0), 1,2-didocosahexaenoyl-*sn*-glycero-3-phosphocholine (PC 22:6/22:6),
128 1,2-dilignoceroyl-*sn*-glycero-3-phosphocholine (PC 24:0/24:0), 1-(1Z-octadecenyl)-2-oleoyl-*sn*-glycero-
129 3-phosphocholine (PLsC p180/18:1, where p refers to the ether-linked alcohol), 1-(1Z-octadecenyl)-2-
130 docosahexaenoyl-*sn*-glycero-3-phosphocholine (PLsC p180/22:6) and mixture PC molecular species
131 of brain porcine.

132 *2.3. Lipid extraction*

133 Eyeballs were collected from a calf as well as from nine human donors according to a previously
134 published procedure [47]. Samples from human cadavers were collected in accordance with the
135 guidelines of the Declaration of Helsinki. Human eyeballs were obtained from 9 donors (bodies
136 donated to science, five women and four men; mean age, 84.3 ± 8.5 years; range, 72–97 years)
137 within 16 h (median time, mean time 15 ± 7 h) after death. The bodies were refrigerated at 4°C in the
138 first hours after death (less than 24 h). Eyeballs were enucleated at the anatomy laboratory of the

4

139 Saint-Etienne School of Medicine (France). Enucleated eyeballs were immersed in balanced salt

140 solution (BSS, Alcon, Rueil Malmaison, France) at 4°C. Within 30 min after enucleation, a circular

141 section at the pars plana was taken with an 18-mm-diameter trephine and the corneoscleral disc

142 removed for other studies. The posterior pole was placed on a back-lit table and the retina was

143 observed under an operating microscope to select the tissue included in this study. Eyes with large

144 drusen or severe pigment epithelial alterations, severe macular atrophy, macular hemorrhage, or any

145 grossly visible chorioretinal pathologic abnormality were excluded. The vitreous body was carefully

146 removed. The entire neural retina was carefully separated with forceps. Samples were stored at -80°C

147 under argon atmosphere. Total lipids were extracted from retinas according to the method described

148 by Folch *et al.* (1957) [48]. The phosphorus content of the total phospholipid extract was determined

149 according to the method developed by Bartlett and Lewis [49]. The total phospholipids were dried

150 under a stream of nitrogen, after which internal standards PC 14:0/14:0 (final concentration, 0.4 ng/μL)

151 and PC 24:0/24:0 (final concentration, 0.64 ng/μL) were added at about 30% of the major PC

152 molecular species. The samples were then diluted to the appropriate concentration of 12.5 ng/μL in

153 chloroform/methanol (1:1, v/v) for analysis and stored at -80°C under argon atmosphere.

154 ### *2.4. LC-ESI-MS using triple-quadrupole mass spectrometer*

155 The total phospholipids were analysed by liquid chromatography coupled to a mass spectrometer

156 equipped with an ESI source. HPLC was performed using a JASCO PU 2089 Plus LC pump equipped

157 with a JASCO AS 2057 Plus auto-sampler from JASCO Analytical Instruments (Bouguenais, France).

158 The injection volume was 5 μL. The separation was performed using a Hypersil Silica Column (150

159 mm × 2.1 mm, i.d. × 3 μm) from ThermoFinnigan (San Jose, CA, USA). The mobile phase consisted

160 of (A) hexane/2-propanol/chloroform/water (44/43.5/10.5/2, v/v/v/v) containing 12.5 mM of ammonium

161 formate and (B) hexane/2-propanol/chloroform/water (34/49/10.5/6.5, v/v/v/v) containing 12.5 mM of

162 ammonium formate. The solvent-gradient system comprised as follows: 0 min A/B (%) 100/0, 10.5–24

163 min A/B (%) 22/78, 26.5–45 min A/B (%) 0/100% and 46–60 min A/B (%) 100/0. The flow rate was 300

164 μL.min^{-1} and the column was maintained at 30°C. The flow from LC was split using an analytical fixed

165 flow splitter (split ratio = 1:1, post-column) from Analytical Scientific Instruments (El Sobrante, CA,

166 USA). Mass spectrometry was performed using a ThermoFinnigan TSQ Quantum triple quadrupole

167 mass spectrometer equipped with a standard electrospray ionisation source outfitted with a 100-μm

168 i.d. H-ESI needle. The source spray head was oriented at a 90° angle orthogonal to the ion-transfer

169 tube. Nitrogen was used for both the sheath and the auxiliary gases. The MS signals of PC species

170 were first optimised by continuous infusion of the standards dissolved in the mobile phase using ESI in

171 negative and positive modes. The electrospray ionisation spray voltages were 3 kV and −4.5 kV in

172 negative and positive ion modes, respectively, vaporiser temperature was 150°C, sheath gas N_2

173 pressure 45 (arbitrary units), auxiliary gas pressure 45 (arbitrary units), ion sweep gas pressure 5, ion

174 transfer capillary temperature 300°C, skimmer offset 5 V and multiplier gain 300,000.

175 When operated under full scan conditions in the negative and positive ion modes, data were collected

176 in the range of *m/z* 400–1100 with a scan time of 0.5 s. For PC characterisation in the negative mode,

177 ESI-MS/MS was used with argon as the collision gas at 1.5 mTor, and the collision energy was set to

5

178   15 eV; in the positive mode, the collision gas pressure was 0.8 mTor and the collision energy ranged

179   from 30 to 45eV. PC species were manually identified with the parent mass information and their

180   characteristic fragment ions in the CID spectrum using lists of PL species prepared in our laboratory.

181   For PC quantification in ESI/MS/MS, precursor scanning at m/z 184 was used. Optimum conditions for

182   collision-induced dissociation (CID) were selected. For all calculations, the ratio of peak area of each

183   PC species to the peak area of the internal standards (PC 14:0/14:0 and PC 24:0/24:0) was used.

184   Corrections are applied to the data for isotopic overlap. The data were processed using the Xcalibur

185   software (ThermoFinnigan).

2.5. Preparation of fatty acid methyl esters

187   The fatty acid methyl esters (FAMEs) were prepared using the boron trifluoride (BF_3) reagent as the

188   catalyst according to Morrison and Smith [50]. Briefly, lipids (up to 20 mg) were transferred to a

189   centrifuge tube with a PTFE-lined screw cap and evaporated under a stream of nitrogen; 0.3 mL of

190   toluene and 0.7 mL of boron trifluoride reagent (BF_3/methanol, 7%) were added under nitrogen and

191   the tube was closed with the screw cap. The tube was then heated to 95°C for 2 h and then cooled to

192   room temperature. FAMEs were extracted by adding 5 mL of saturated solution of $NaHCO_3$ and 3×2

193   mL of hexane. The mixture was centrifuged (3000 rpm) for 3 min to break the emulsion formed. After

194   drying the organic phase over sulfate sodium (Na_2SO_4), the solvent was removed under a stream of

195   nitrogen and FAMEs were dissolved in hexane for GC analysis.

2.6. Gas-chromatography analysis

197   FAMEs (0.5 mg/mL in hexane) were analysed on a Hewlett Packard Model 4890 gas-chromatograph

198   (Palo Alto, CA, USA) using a CP-Sil 88 (100 m × 0.25 mm I.D. capillary column, 0.2 μm film, Varian,

199   Courtaboeuf, France). The instrument was equipped with a split/splitless injection (splitless for 0.5

200   min). The linear velocity of hydrogen was 37.0 cm/s at 60°C. The temperature was held at 60°C for 5

201   min, raised to 165° at 15°C/min and held for 1 min and then to 225°C at 2°/min and finally held at

202   225°C for 17 min according to the procedure described in the literature [51]. The injection port was

203   held at 250°C and a flame ionisation detector (FID) was used at 250°C.

2.7. Preparation of 4,4-dimethyloxazoline derivatives

205   FAME (up to 2 mg) were converted to the 4,4-dimethyloxazoline (DMOX) derivatives by treatment with

206   250 μL of 2-amino-2-methyl-1-propanol in a test tube at 170°C overnight in a nitrogen atmosphere

207   [52]. The reaction mixture was cooled and dissolved in 3 mL of dichloromethane and further washed

208   twice with 5 mL of water. After drying the organic phase over Na_2SO_4, the solvent was removed under

209   a stream of N_2 and the sample was dissolved in hexane for GC-MS analysis.

2.8. Gas-chromatography mass-spectrometry

211   GC-MS analyses of DMOX derivatives were carried out on an Agilent 6890 series II gas

212   chromatograph attached to an Agilent model 5973N selective quadrupole mass detector (Palo Alto,

213   CA, USA) operating in the electronic ionisation mode under an ionisation voltage of 70 eV at 230°C.

214   Agilent ChemStation software was used for data acquisition and processing. The injector (splitless

6

215 mode) and the interface temperature were maintained at 250°C, whereas helium was used as the
216 carrier gas under constant flow at 1 mL/min. Spectral data were acquired over a mass range of 50–
217 600 amu. GC separation was performed on a BPX-70 (60 m × 0.25 mm I.D. capillary column, 0.25 µm
218 film; SGE, Melbourne, Australia). The temperature was held at 60°C for 1 min, raised to 240 at
219 20°C/min and held at 240°C for 90 min.

220 **3. Results and discussion:**

221 The objective of the present study was to develop a sensitive and specific method for the
222 characterisation and quantification of PC species and in particular VLC-PC species in human retina
223 using LC-ESI-MS/MS. Given the greater availability of bovine retinas compared to human retinas, the
224 former were used by means of characterisation of VLC-PC. Bovine retina is also known to contain
225 VLC-PUFA (C24–C36), specifically concentrated in PC [2].

226 *3.1. Separation of phospholipid classes*

227 We chose to separate the phospholipid species using LC prior to the ESI-MS/MS analysis in order to
228 enhance the detection of the minor isobaric species in the mixture. Additionally, a suitable
229 chromatographic separation may reduce any ESI suppression of non-isobaric and co-eluting species.
230 Then we developed a normal-phase HPLC separation of phospholipid (PL) classes in order to
231 separate and study the collision-induced dissociation of these PC molecular species containing VLC-
232 PUFA using a triple-quadrupole instrument.

233 Phospholipid species are zwitterionic molecules. Therefore either positive- or negative-ion mass
234 spectra of these phospholipid classes were accessible through ESI-MS analysis. However, negative-
235 ion ESI mass spectra of phosphatidylethanolamine (PE), lyso-phosphatidylethanolamine (LPE),
236 phosphatidylinositol (PI) and phosphatidylserine (PS) species only contain the $[M-H]^-$ ion and were far
237 more sensitive than positive-ion spectra [20]. In contrast, PC, lyso-phosphatidylcholine (LPC) and
238 sphingomyelin (SM) species were more efficiently analysed in the positive-ion mode by generating
239 protonated $[M+H]^+$ ions but might also produce sodiated adduct $[M+Na]^+$ ions. Only during the
240 development of LC separation of total phospholipids was the mass spectrometer operated under full
241 scan conditions in the negative ion mode for detection of PE, PI, PS and LPE and under full scan
242 conditions in the positive ion mode for quantification of PC, LPC and SM species. A mobile phase
243 consisting of hexane/isopropanol/chloroform/water for HPLC separation of PL classes on silica
244 columns has been reported to give good separation for some PLs [53,54]. However, since PI and PS
245 as well as PC and SM eluted very closely, class determination was far more complicated. In our study,
246 ammonium formate was added to this mobile phase system to enhance separation, resolution and
247 selectivity. By optimising the concentration of ammonium formate in the mobile phase, the flow rate
248 and the use of a pertinent gradient, a good baseline separation of PE, PI, PS, PC, SM and LPC
249 classes in bovine and human retinas was achieved, as illustrated in **Fig. 1**. The method did not require
250 fractionation into neutral lipids and phospholipids. Total lipid extracts from retinas can be injected
251 directly into the system, with neutral lipids eluting with the solvent front. As expected,
252 plasmenylcholine (PlsC) species co-eluted with PC species. Moreover, under our HPLC conditions,
253 VLC-PC molecular species containing VLC-PUFA eluted separately just before other PC molecular

7

254 species, between 15.5 and 17 min. Also, it was possible to collect this fraction in order to concentrate

255 VLC-PC for further structure characterisation using GC-MS.

3.2. Determination of PC species based on their specific fragmentation mechanisms

257 Detailed structural analysis of glycerophospholipids can be performed using electrospray tandem

258 mass spectrometry (ESI-MS/MS). Collision-induced dissociation (CID) of $[M+H]^+$ or $[M-H]^-$ of

259 phospholipids results in fragment ions that are related to the polar head group and fatty acyl

260 substituent esterified to the glycerol backbone.

261 In order to characterise PC molecular species, lipid extracts from bovine retina were analysed by ESI-

262 MS/MS in the positive and negative modes. Mass spectra obtained by CID of PC molecular ions were

263 compared with those obtained from commercial standards. When operated in the single-stage MS

264 mode using ESI in the positive ionisation mode, PC molecular species produced abundant $[M+H]^+$ ions

265 as well as sodiated $[M+Na]^+$ ions [18]. The MS^2 fragmentation of the selected $[M+H]^+$ molecular ion of

266 PC and PlsC gave an intense fragment at *m/z* 184 derived from phosphocholine head $[C_5H_{13}NPO_4]^+$.

267 When operated in the single-stage MS mode in the negative mode ionisation, PC molecular species

268 produced abundant demethylated molecule $[M – CH_3]^-$ ions (base peak). Molecular ions $[M-H]^-$ were

269 not detected. Under our HPLC conditions with chloroform and ammonium formate, chloride- $[M+Cl]^-$

270 and formate- $[M+HCOO]^-$ adducts were also produced. By increasing the skimmer-off set value from 5

271 to 25 V, it was possible to reduce these two adducts. The MS^2 experiment of the selected $[M – CH_3]^-$

272 of PC species gave a characteristic fragmentation. As an example, for PC 16:0/18:1 **(Fig. 2A)**, the

273 MS^2 fragmentation of the selected molecular ion $[M – CH_3]^-$ at *m/z* 744 showed two prominent ions

274 derived from the carboxylate anions at *m/z* 281 (major) and *m/z* 255 (minor), which correspond to the

275 C18:1 and C16:0 fatty acyl substituent, respectively. Elimination of the fatty acyl substituent C18:1 and

276 C16:0 leads to the formation of very minor fragments at *m/z* 462 and *m/z* 488, corresponding to the [M

277 $– CH_3 – R_2CHCOOH]^-$ and the $[M – CH_3 – R_1CHCOOH]^-$ ions respectively. Two other fragments at

278 *m/z* 480 and *m/z* 506 were also detected in slightly greater amounts than fragments at m/z 462 and

279 m/z 488. These fragments corresponded to the $[M – CH_3 – R_2CH=C=O]^-$ and the $[M – CH_3 –$

280 $R_1CH=C=O]^-$ ions, respectively, resulting from the loss of fatty acyl groups such as ketenes [19,21].

281 According to some authors, acyl chain distribution in phospholipids can be accurately determined with

282 a triple-quadrupole spectrometer. The intensity of the carboxylate anion derived from the *sn*-2 acyl

283 substituent is greater than the carboxylate anion derived from the *sn*-1 acyl substituent [18,19].

284 However, under our conditions, it was not verified with PC containing an LC-PUFA in position *sn*-2,

285 e.g. C20:4n-6 **(Fig. 2B)** or C22:6n-6 **(Fig. 2C)**. Indeed when R_2CH_2COOH was an LC-PUFA, a

286 fragment was also detected at a mass 44 Da lower than the carboxylate anion $[R_2CH_2COO]^-$. This

287 fragment is generated by the loss of one CO_2 molecule from this LC-PUFA carboxylate anion. For

288 example, the MS^2 fragmentation of the selected molecular ion $[M-CH_3]^-$ at *m/z* 794 of PC 18:0/20:4

289 showed two prominent ions at *m/z* 283 (C18:0 carboxylate anion) and *m/z* 303 (C20:4 carboxylate

290 anion) and a lower fragment at *m/z* 259 generated by CO_2 loss by the C20:4 carboxylate anion. In the

291 case of PC 18:0/22:6, the fragment at *m/z* 327 was decreased by the loss of one CO_2 molecule from

292 the C22:6 carboxylate anion, while the fragment at *m/z* 283 was increased because it was the sum of

8

293　two fragments: the C18:0 carboxylate anion and the ion formed by the loss of 44 Da from the C22:6

294　carboxylate anion. Consequently, the intensity of the C18:0 carboxylate anion derived from the *sn*-1

295　acyl substituent was greater than the C22:6 carboxylate anion derived from the *sn*-2 acyl substituent.

296　In contrast, the regiospecificity of the acyl moieties in asymmetrical PC, even with a LC-PUFA in the

297　*sn*-2 position, can be confirmed from the packet of *sn*-1 acyl and *sn*-2 acyl lyso-PC product-ion peaks

298　because the *sn*-1 acyl lyso-PC ion is always more abundant than the *sn*-2 acyl lyso-PC ion (**Fig. 2A–**

299　**C**) [19]. For plasmalogen species, only the carboxylate anion corresponding to the *sn*-2 acyl

300　substituent was detected, since the *sn*-1 substituent did not easily cleave to form an anion [19,35] (**Fig**

301　**2D**). However, in the case of PlsC 18:0/22:6 **(Fig. 2E)**, the MS^2 fragmentation of the selected

302　molecular ion [M – CH_3]$^-$ at *m/z* 802 shows the ion at *m/z* 327 corresponding to the C22:6 carboxylate

303　anion and the fragment at *m/z* 283, which is generated by CO_2 loss, as explained above. Thus, during

304　the interpretation of spectra from PC or PlsC containing C22:6n-3 in the *sn-2* position, it is important to

305　pay attention to the fragment at *m/z* 283 generated by CO_2 loss by C22:6 carboxylate anion, because

306　it can be confused with the C18:0 carboxylate anion.

307　The PC species were characterised in bovine retina. The different PC, VLC-PC and PlsC molecular

308　species characterised in bovine retina (**Fig. 3A**) are listed in Table 1. We particularly focused on the

309　VLC-PC fraction in the retina (**Fig. 3B**). Identification by ESI-MS/MS showed that this fraction

310　contained exclusively dipolyunsaturated PC species with one VLC-PUFA always in the *sn*-1 position

311　and docosahexaenoic acid (DHA, C22:6n-3) exclusively at the *sn*-2 position. For example, as

312　illustrated in **Fig. 2F** the product ion spectra of the demethylated molecular ion [M – CH_3]$^-$ of PC

313　32:4/22:6 at *m/z* 1006 showed the two abundant ions at *m/z* 327 and *m/z* 471, corresponding to C22:6

314　and C32:4 carboxylate anions, respectively, and the ion at *m/z* 283, which is generated by CO_2 loss by

315　the C22:6 carboxylate anion. Furthermore, we observed the product ions formed by neutral loss of

316　either an FA or a ketene at *m/z* 678 ([M – CH_3 – R_2CH-$COOH$]$^-$), *m/z* 696 ([M – CH_3 – R_2CH=C=O]$^-$),

317　and *m/z* 552 ([M – CH_3 – R_1CH=C=O]$^-$). Among these three fragments, the fragment at *m/z* 696 was

318　the most abundant and it was therefore useful for regioisomeric assignment.

319　We characterised 69 PC molecular species, in particular 22 VLC-PC molecular species, in bovine

320　retina (**Table 1**). All these identified VLC-PC molecular species contained C22:6 in the *sn*-2 position

321　and VLC-PUFA in the sn-1 position according to Aveldaño [55]. These VLC-PC species contained

322　fatty acyl from 24 to 36 carbon chains long, with four, five or six double bonds. The majority of VLC-PC

323　contained C32 and C34 VLC-PUFA with four, five or six double bonds. Phospholipids from human

324　retina were also separated (**Fig. 1B**) using the same LC-ESI-MS conditions. The main PC and VLC-

325　PC were characterised and compared to those identified in bovine retina (**Fig. 4**). Thirty-six PC

326　molecular species and in particular 13 VLC-PC molecular species were detected in significant

327　amounts in human retina (**Table 2**). Similar structures of VLC-PC to those in bovine retina were

328　characterised in human retina. C22:6 still remained in the *sn*-2 position and the VLC-PUFA in the *sn*-1

329　position. Moreover, as in bovine retina, the majority of VLC-PC contained C32 and C34 VLC-PUFA

330　with four, five or six double bonds. Only traces of VLC-PC containing C30:5, C30:6, C36:5 and C36:6

331　were also detected but could not be quantified.

9

332   For structural identification of VLC-PUFA, LC-MS/MS did not allow localisation of the double bonds

333   along the carbon chain. According to previous studies, retinal C28-C36 fatty acids are polyunsaturated

334   and belong to the n-3 and n-6 families [2,56]. The n-6 family of C28-C36 fatty acids has four or five

335   double bonds, while the n-3 family of VLC-PUFA contain five or six double bonds. To check these in

336   our retina samples, a part of the isolated VLC-PC fraction by HPLC was converted into fatty acid

337   methyl esters (FAMEs) and analysed by GC-FID). An aliquot of FAME of the isolated VLC-PC fraction

338   from bovine retina was then converted into DMOX derivative and analysed using GC-EI-MS (**Fig. 5A**).

339   Identification was established according to previous studies [52,57,58]. For example, the mass spectra

340   of the DMOX derivative of C32:4 (n-6) and C32:6 (n-3) are presented in **Fig. 6**. GC-MS mass spectra

341   of DMOX derivative of C32:6 n-3 and 32:4 n-6 gave intense molecular ions at m/z 521 and m/z 525

342   respectively, and fragmentation localised the double bonds in the carbon chain. In DMOX derivatives

343   of mono- or polyunsaturated fatty acids, a mass interval of 12 amu instead of the regular 14 amu

344   between two neighbouring homologous fragments containing n-1 and n carbon atoms of the original

345   acid moiety indicates that a double bond exists between carbons n and n+1 in the chain [58].

346   Moreover, it is important to note that a gap of 40 amu is also observed between the two fragments

347   containing n-2 and n+1 carbon atoms, located around the double bond. Thus, we have established the

348   mass spectra of the DMOX derivatives of major VLC-PUFA detected in the isolated VLC-PC fraction

349   obtained by HPLC from bovine and human retinas (**Fig. 6A and 6B**). In our samples of bovine retinas,

350   as in human retinas, C30-C34 VLC-PUFA of the n-6 family had only four double bonds, while C28-

351   C36 VLC-PUFA of the n-3 family had five or six double bonds. Moreover, as expected, C32 and C34

352   VLC-PUFA with four, five and six double bonds seem to represent the prominent VLC-PUFA in bovine

353   retinas as well as in human retinas. These results are in agreement with our LC-MS/MS data.

354   PUFA longer than C26 are suspected of having key functions in several tissues. For example, they are

355   essential components of epidermal acylceramides and then important actors in skin barrier function

356   [59,60], whereas they were shown to be involved in sperm maturation in testis [61,62]. In the retina,

357   C28-C36 VLC-PUFA appear to be associated with rhodopsin in photoreceptor outer segments [55]

358   and are suspected of being involved in phototransduction processes. This hypothesis is consistent

359   with the electroretinographic defects in the various mouse models carrying various mutations in the

360   *ELOVL4* gene [13,63-65], even if their retinas have not been fully characterised in terms of changes in

361   C28-C36 acyl PCs.

362   ***3.3. Quantification of the PC species in total lipids extracted from human retina***

363   In single-stage positive-ion ESI-MS of total lipid extracts, PC molecular species often give rise to major

364   peaks corresponding to the sodiated molecular ions [M+Na]$^+$ along with the protonated ones [M+H]$^+$.

365   This phenomenon, also reported previously [17-19,36], complicates the analysis of PCs in biological

366   samples. Addition of ammonium formate in the LC solvent considerably reduced the formation of

367   sodiated adducts [M+Na]$^+$ (<5%) but did not eliminate them completely [31]. Alternatively, some

368   authors included sodium or lithium salts to suppress formation of protonated ions [19,66]. However,

369   we were not able to avoid protonated ions by post-column inclusion of lithium or sodium salts, directly

370   in the source. In the MS^2 mode, PC species showed an intense fragment at m/z 184 due to their

10

371 choline head group. This fragment was used for precursor ion scanning, whereby the [M+H]$^+$ ions of

372 PCs are specifically detected [29,30,36]. Precursor ion scanning for *m/z* 184 selectively detects only

373 [M+H]$^+$ ions for choline-containing phospholipids, since PC molecules cationised by sodium or

374 potassium exclusively lose their polar choline phosphate head group as a 183-Da neutral fragment

375 instead of forming the fragment at *m/z* 184 [34]. To optimise the formation of this precursor, we

376 investigated the influence of the fatty acid chain length on the intensity and optimal collision cell offset

377 for the generation of the *m/z* 184 fragment for PC 14:0/14:0 (PC 28:0), PC 16:0/16:0 (PC 32:0), PC

378 18:0/18:0 (PC 36:0), PC 20:0/20:0 (PC 40:0), PC 23:0/23:0 (PC 46:0), PC 24:0/24:0 (PC 48:0), PC

379 16:0/18:1(PC 34:1), PC 18:0/18:2 (PC 36:2), PC 18:0/20:4 (PC 38:4), PC 18:0/22:6 (PC 40:6), PC

380 22:6/22:6 (PC 44:12) and PlsC 18:0/22:6 (PlsC 40:6). Collision cell offset plots were established

381 correlating the fragment ion intensity at *m/z* 184 with the voltage off in the collision cell. Moreover,

382 collision cell offset plots were also established for the more intense VLC-PUFA, PC 32:4/22:6 (PC

383 54:10, m/z 1022) and PC 34:4/22:6 (PC 56:10, m/z 1050) using the isolated and concentrated HPLC

384 fraction containing VLC-PC. As a result, the optimal collision offset increases with increasing chain

385 length, varying from about −30 to −50 V for the precursor ions investigated. As a compromise, −36 V

386 was selected as collision cell offset.

387 Determination of phospholipid molecule species level requires the addition of internal standards

388 because the ionisation efficiency between different phospholipid classes of ESI-MS may differ

389 significantly with respect to experimental conditions. PC 14:0/14:0 (*m/z* 678) and PC 24:0/24:0 (*m/z*

390 958) were selected as internal standards in the analyses of PC, PlsC and VLC-PC since these

391 molecular species do not occur naturally in biological samples studied in this work. However,

392 precautions were taken in this quantitative study because different molecular species are not detected

393 with equal efficiency. Previous studies indicated that the total phospholipid concentration affect the

394 quantification of PC species by ESI-MS/MS [29]. Therefore, we investigated the influence of these

395 different parameters on the instrument response. First, to establish the range of linear response of our

396 ESI-MS/MS instrument, an equimolar mixture was prepared with standards of PC 14:0/14:0, PC

397 16:0/16:0, PC 16:0/18:1, PC 18:0/18:0, PC 18:0/18:2, PC 18:0/20:4, PC 18:0/22:6, PlsC 18:0/22:6, PC

398 20:0/20:0, PC 22:6/22:6, PC 23:0/23:0 and PC 24:0/24:0, diluted from 5 pg/μL to 5 ng/μL per species

399 (from 60 pg/μL to 60 ng/μL of total PC) in chloroform/methanol (1:1) and then injected to LC-ESI-MS.

400 The PC mixture had a linear response of ion count versus concentration from 5 pg to 2 ng/μL (from 60

401 pg/μL to 24 ng/μL of total PC) (**Fig. 7**). Beyond this concentration, the response was nonlinear and

402 began to plateau.

403 Furthermore, the acyl chain length and chain unsaturation have a significant effect on the instrument

404 response [28,34,36,67]. We established a calibration curve between the intensity of the observed

405 quasi-molecular ion species and the length and degree of unsaturation of the carbon chains.

406 Response curves were prepared with increased concentrations of PC 16:0/16:0, PC 16:0/18:1, PC

407 18:0/18:2, PC 18:0/18:0, PC 18:0/20:4, PC 18:0/22:6, PlsC 18:0/22:6, PC 20:0/20:0, PC 22:6/22:6 and

408 PC 23:0/23:0 (range, 2.5 pg/μL to 2.5 ng/μL) and fixed concentrations of PC14/14:0 (0.4 ng/μL) and

409 PC 24:0/24:0 (0.64 ng/μL) as internal standards. Linear calibration curves were obtained for PC

410 species from 2.5 pg/μL to 2.5 ng/μL. Our results confirmed that the instrument response for PC

11

411 species decreases when the phospholipid acyl chain length is increased [28,34,36]. According to

412 Koivusalo et al. [36], the responses remain a linear function of the acyl chain length, even at the

413 highest concentrations. Lastly, under our conditions, the effect of acyl chain unsaturation seems to be

414 weak. Previous studies showed that the effect of acyl chain unsaturation was less significant when the

415 injection amount of lipid molecules is minimised [27,36]. To overcome this problem, experiments were

416 conducted with the least amount of required material.

417 After having determined the effect of structural factors and lipid concentration on the instrument, we

418 used this information to quantify the molecular species of PC and PlsC in human retina. In order to

419 check the applicability of the method in a biological sample, samples of human retina (12.5 ng/µL) or

420 blank (chloroform/methanol) were spiked with the increment level of an equimolar mixture of saturated

421 PC 14:0/14:0, PC 18:0/18:0, PC 20:0/20:0, PC 23:0/23:0 and PC 24:0/24:0 (0.25, 0.5 or 1 ng/µL per

422 species), and then analysed. An example of representative spectrum is shown in **Fig. 8**. These

423 allowed us to correct for acyl chain length dependency of the instrument response. Consequently, a

424 calibration function was then calculated and used to correct the experimental ion abundance in order

425 to obtain the true molar abundance. With VLC-PUFA (from PC 52:9 and PC 58:10), no standards were

426 available to calculate the calibration curve. Therefore, this curve was extrapolated from the different

427 results obtained above as a function of the phospholipid acyl chain length and the degree of acyl chain

428 unsaturation.

429 The calibration method developed was then applied to quantify PC and VLC-PC molecular species

430 extracted from retina samples obtained from nine human donors. The phosphorus content of total lipid

431 extracts was determined using the Bartlett and Lewis method [49] in order to standardise the

432 concentration of all lipid extracts at 12.5 ng/µL. A constant amount of both PC 14:0/14:0 (0.4 ng/µL)

433 and PC 24:0/24:0 (0.64 ng/µL) were therefore added to an aliquot of the lipid extract (12.5 ng/µL) for

434 the quantification. PC 24:0/24:0 was added with a known amount in order to estimate the accuracy of

435 the MS method for every sample. The identified and quantified 36 PC species in human retinas are

436 listed in **Table 2**. In most of these, 13 VLC-PUFA-containing dipolyunsaturated PC were detected and

437 quantified. The main VLC-PC (PC containing VLC-PUFA) detected and quantified in human neural

438 retinas were those having VLC-PUFA of 32 carbon atoms (C32:3, C32:4, C32:5 and C32:6) and 34

439 carbon atoms (C34:3, C34:4, C34:5 and C34:6). Dipolyunsaturated PC with 30:5, 30:6, 36:5 and 36:6

440 were detected but in smaller quantities.

441 **4. Conclusion**

442 In summary, qualitative and quantitative analysis of VLC-PC species was examined in this paper. An

443 accurate method using normal-phase HPLC coupled on-line with triple quadrupole mass spectrometer

444 was developed to characterise and quantify all PC species, including VLC-PCs in human retina and

445 bovine retinas. Since the results from molecular and biochemical studies led to the conclusion that

446 VLC-PUFA are involved in the pathogenesis of STD3, the method developed herein may be useful to

447 more accurately investigate the molecular mechanisms leading to photoreceptor dysfunction and

448 death in STD3.

449

12

453   **References**

454   [1]   M.I. Aveldano, J. Biol. Chem. 262 (1987) 1172.
455   [2]   M.I. Aveldano, H. Sprecher, J. Biol. Chem. 262 (1987) 1180..
456   [3]   A. Poulos, Lipids 30 (1995) 1.
457   [4]   N.P. Rotstein, M.I. Aveldano, Biochem. J. 249 (1988) 191.
458   [5]   N.P. Rotstein, M.I. Aveldano, Biochem J. 249 (1988) 191.
459   [6]   Z.Q. Zhang, Y. Wang, H.G. Vikis, L. Johnson, G.J. Liu, J. Li, M.W. Anderson, R.C. Sills, H.L.
460   Hong, T.R. Devereux, T. Jacks, K.L. Guan, M. You, Na. Genet. 29 (2001) 25.
461   [7]   A.O. Edwards, L.A. Donoso, R. Ritter, Invest. Ophthalmol. Vis. Sci. 42 (2001) 2652.
462   [8]   C. Grayson, R.S. Molday, J. Biol. Chem. 280 (2005) 32521.
463   [9]   P. Tvrdik, R. Westerberg, S. Silve, A. Asadi, A. Jakobsson, B. Cannon, G. Loison, A.
464   Jacobsson, J. Cell Biol. 149 (2000) 707.
465   [10]   A. Meyer, H. Kirsch, F. Domergue, A. Abbadi, P. Sperling, J. Bauer, P. Cirpus, T.K. Zank, H.
466   Moreau, T.J. Roscoe, U. Zahringer, E. Heinz, J. Lipid Res. 45 (2004) 1899.
467   [11]   R. Westerberg, P. Tvrdik, A.B. Unden, J.E. Mansson, L. Norlen, A. Jakobsson, W.H. Holleran,
468   P.M. Elias, A. Asadi, P. Flodby, R. Toftgard, M.R. Capecchi, A. Jacobsson, J. Biol. Chem. 279
469   (2004) 5621.
470   [12]   J.P. SanGiovanni, E.Y. Chew, Prog. Retin. Eye Res. 24 (2005) 87.
471   [13]   G. Karan, C. Lillo, Z. Yang, D.J. Cameron, K.G. Locke, Y. Zhao, S. Thirumalaichary, C. Li,
472   D.G. Birch, H.R. Vollmer-Snarr, D.S. Williams, K. Zhang, Proc. Natl. Acad. Sci. U S A 102
473   (2005) 4164.
474   [14]   A. McMahon, W. Kedzierski, Br. J. Ophthalmol..
475   [15]   M. Agbaga, R.S. Brush, M.N. Mandal, A., K. Henry, M.H. Elliott, R. Anderson, PNAS 105
476   (2008) 12843.
477   [16]   S.S. Antollini, M.I. Aveldano, J. Lipid Res. 43 (2002) 1440.
478   [17]   J.L. Kerwin, A.R. Tuininga, L.H. Ericsson, J Lipid Res. 35 (1994) 1102.
479   [18]   J. Fang, M.J. Barcelona, J. Microbiol. Methods. 33 (1998) 23.
480   [19]   X. Han, R.W. Gross, J. Am. Soc.Mass Spectro. 6 (1995) 1202.
481   [20]   X. Han, W.G. Richard, Proceedings of the National Academy of Sciences of the United States
482   of America 91 (1995) 10635.
483   [21]   T. Houjou, K. Yamatani, H. Nakanishi, M. Imagawa, T. Shimizu, R. Taguchi, Rap. Com. Mass
484   Spectom. 18 (2004) 3123.
485   [22]   C. Beermann, M. Mobius, N. Winterling, J.J. Schmitt, G. Boehm, lipids 40 (2005) 211.
486   [23]   A. Larsen, S. Uran, P.B. Jacobsen, T. Scotland, Rap. Com. Mass Spectom. 15 (2001) 2393.
487   [24]   G. Issac, D. Bylund, J.-E. Mansson, K.E. Markides, J. Bergquist, J. Neurosci. Methods. 128
488   (2003) 111.
489   [25]   A. Carrier, J. Parent, S. Dupuis, J. Chromatogr. A 876 (2000) 97.
490   [26]   B. Barroso, R. Bischoff, J. Chromatogr. B 814 (2005) 21.
491   [27]   E.J. Ahn, H. Kim, B. Chul Chung, G. Kong, M.H. Moon, J. Chromatogr. A 1194 (2008) 90.
492   [28   E.J. Ahn, H. Kim, B.C. Chung, M.H. Moon, J. Sep. Sci. 30 (2007) 2598.
493   [29]   C.J. Delong, P.R. Baker, M. Samuel, Z. Cui, M.J. Thomas, J. Lipid Res. 42 (2001) 1959.
494   [30]   W.D. Lehmann, M. Koester, E. G., K. Dietrich, Anal. Biochem. 246 (1997) 102.
495   [31]   N. Acar, O. Berdeaux, P. Juaneda, S. Gregoire, S. Cabaret, C. Joffre, C.P. Creuzot-Garcher,
496   L. Bretillon, A.M. Bron, Exp. Eye Res. (2009) 840.
497   [32]   M. Malavolta, F. Bocci, E. Boselli, N.G. Frega, J. Chromatogr. B 810 (2004) 173.
498   [33]   K.Z. Berry, R.C. Murphy, J. Am. Soc. Mass Spectrom. 15 (2004) 1499.
499   [34]   B. Brugger, G. Erben, R. Sandhoff, F.T. Wielland, W.D. Lehmann, Proceedings of the National
500   Academy of Sciences of the United States of America 94 (1997) 2339.
501   [35]   F. Gao, X. Tian, W. Dawei, J. Liao, T. Wang, H. Liu, Biochim. Biophys. Acta 1761 (2006) 667.
502   [36]   M. Koivusalo, P. Haimi, L. Heikinheimo, R. Kostiainen, P. Somerharju, J. Lipid Res. 42 (2001)
503   663.
504   [37]   H. Kim, H.K. Min, G. Kong, M.H. Moon, Anal. Bioanal. Chem. 393 (2009) 1649.
505   [38]   H. Kim, E.J. Ahn, M.H. Moon, Analyst 133 (2008) 1656.
506   [39]   X. Han, R.W. Gross, Mass. Spectrom. Rev. 24 (2005) 367.

13

507 [40] M. Pulfer, R.C. Murphy, Mass. Spectrom. Rev. 22 (2003) 332.
508 [41] X. Han, R.W. Gross, J. Lipid Res. 44 (2003) 1071.
509 [42] H. Kim, T.-C. Wang, L., Y.-C. Ma, Anal. Chem. 66 (1994) 3977.
510 [43] M. Hermansson, A. Uphoff, R. Käkelä, P. Somerharju, Anal. Chem. 77 (2005) 2166.
511 [44] R. Taguchi, J. Hayakawa, Y. Takeuchi, M. Ishida, J. Mass. Spectrom. 35 (2000) 953.
512 [45] T. Houjou, K. Yamatani, M. Imagawa, T. Shimizu, R. Taguchi, Rap. Com. Mass Spectrom. 19
513   (2005) 654.
514 [46] D.N. Heller, R.J. Cotter, C. Fenselau, Anal. Chem. 59 (1987) 2806.
515 [47] L. Bretillon, G. Thuret, S. Gregoire, N. Acar, C. Joffre, A.M. Bron, P. Gain, C.P. Creuzot-
516   Garcher, Exp. Eye Res. 87 (2008) 521.
517 [48] J. Folch, M. Lees, G.H.S. Standley, J. Biol. Chem. 226 (1957) 497.
518 [49] E.M. Bartlett, D.H. Lewis, Anal. Biochem. 36 (1970) 159.
519 [50] W.R. Morrison, L.M. Smith, J. Lipid Res. 5 (1964) 600.
520 [51] F. Dionisi, P.A. Golay, L.B. Fay, Anal. Chim. Acta 465 (2002) 395.
521 [52] L. Fay, U. Richli, J. Chromatogr. 541 (1991) 89.
522 [53] P. Juaneda, G. Rocquelin, P.O. Astorg, Lipids 25 (1990) 756.
523 [54] W.W. Christie, J. Lipid Res. 26 (1985) 507.
524 [55] M.I. Aveldano, Biochemistry 27 (1988) 1229.
525 [56] M. Such, A.A. Wierzbicki, M.T. Clandinin, Biochim. Biophys. Acta -Lipids and Lipid Metabolism
526   1214 (1994) 54.
527 [57] O. Berdeaux, R. Wolff, J. Am. Oil Chem. Soc. 73 (1996) 1323.
528 [58] J.Y. Zhang, Q.T. Yu, B.N. Liu, Z.H. Huang, Biomed. Environ. Mass Spectrom. 15 (1988) 33.
529 [59] D.J. Cameron, Z.Z. Tong, Z.L. Yang, J. Kaminoh, S. Kamiyah, H.Y. Chen, J.X. Zeng, Y.L.
530   Chen, L. Luo, K. Zhang, Int. J. Biol. Sci. 3 (2007) 111.
531 [60] V. Vasireddy, Y. Uchida, N. Salem, S.Y. Kim, M.N.A. Mandal, G.B. Reddy, R. Bodepudi, N.L.
532   Alderson, J.C. Brown, H. Hama, A. Dlugosz, P.M. Elias, W.M. Holleran, R. Ayyagari, Hum.
533   Mol. Genet. 16 (2007) 471.
534 [61] N.E. Furland, E.N. Maldonaldo, M.I. Aveldano, Lipids 38 (2003) 73.
535 [62] M. Rabionet, A.C. van der Spoel, C.C. Chuang, B. von Tumpling-Radosta, M. Litjens, D.
536   Bouwmeester, C.C. Hellbusch, C. Korner, H. Wiegandt, K. Gorgas, F.M. Platt, H.J. Grone, R.
537   Sandhoff, J. Biol. Chem. 283 (2008) 13357.
538 [63] V. Vasireddy, M.M. Jablonski, M.N. Mandal, D. Raz-Prag, X.F. Wang, L. Nizol, A. Iannaccone,
539   D.C. Musch, R.A. Bush, N. Salem, Jr., P.A. Sieving, R. Ayyagari, Invest. Ophthalmol. Vis. Sci.
540   47 (2006) 4558.
541 [64] D. Raz-Prag, R. Ayyagari, R.N. Fariss, M.N. Mandal, V. Vasireddy, S. Majchrzak, A.L.
542   Webber, R.A. Bush, N. Salem, Jr., K. Petrukhin, P.A. Sieving, Invest. Ophthalmol. Vis. Sci. 47
543   (2006) 3603.
544 [65] W. Li, Y. Chen, D.J. Cameron, C. Wang, G. Karan, Z. Yang, Y. Zhao, E. Pearson, H. Chen, C.
545   Deng, K. Howes, K. Zhang, Vision Res. 47 (2007) 714.
546 [66] F.F. Hsu, A. Bohrer, J. Turk, J. Am. Soc. Mass Spectrom. 9 (1997) 516.
547 [67] C.Y. Lee, A. Lesimple, A. Larsen, O. Mamer, J. Genest, J. Lipid Res. 46 (2005) 1213.

548
549 **Figures legends:**

550 **Figure 1:** (A) LC-ESI-MS normal-phase chromatogram of the lipid extract from bovine retina. The

551 retention time of phosphatidylethanolamine (PE), phosphatidylinositol (PI), phosphatidylserine (PS),

552 phosphatidylcholine (PC), sphingomyelin (SM), and lyso-phosphatidylcholine (LPC) classes were 7–

553 8.5 min, 11–12 min, 12–14 min, 15.5–22 min, and 23–27.5 min, respectively. (B) LC-ESI-MS normal-

554 phase chromatogram of the lipid extract from human retina. The retention time of PE, PI,PS, PC, SM,

555 and LPC classes were 7–8 min, 11–12 min, 13–14 min, 15.6–21 min and 23.5–27 min, respectively.

556 The mass spectrometer was operated under full scan in the negative ion mode from 0 to 15 min and in

557 the positive ion mode from 15 min to 40 min.

558 **Figure 2:** Product-ion spectra of negative ions of various commercial phosphatidylcholines (PC)

559 (collision offset, +25 V). (A) Product ion spectrum of the [M – CH$_3$]$^-$ of PC 16:0/18:1 at *m/z* 744. (B)

560 Product ion spectrum of the [M – CH$_3$]$^-$ of PC 18:0/20:4 at *m/z* 794. (C) Product ion spectrum of the [M

14

561 – CH$_3$]$^-$ of PC 18:0/22:6 at *m/z* 818. (D) Product ion spectrum of the [M – CH$_3$]$^-$ PlsC 18:0/18:1 at *m/z*

562 756. (E) Product ion spectrum of the [M – CH$_3$]$^-$ PlsC 18:0/22:6 at *m/z* 802. (F) Product ion spectrum

563 of the [M – CH$_3$]$^-$ of PC 32.4/22:6 at *m/z* 1006.

564 **Figure 3:** Negative-ion HPLC-ESI-MS analysis of phosphatidylcholine (PC) molecular species from

565 bovine retina. The mass spectrometer was operated under full scan from 650 to 1100 uma. (A) Mass

566 spectrum of total PC fraction including PC-containing VLC-PUFA (VLC-PC) collected from 15.2 min to

567 22 min, as shown in Figure 1; (B) mass spectrum of VLC-PC fraction from 15.2 min to 16.8 min, as

568 shown in Figure 1.

569 **Figure 4:** Negative-ion HPLC-ESI-MS mass spectrum of total phosphatidylcholine (PC) fraction

570 including PC-containing VLC-PUFA (VLC-PC) collected from 15.6 min to 21 min, as shown in Figure

571 6. The mass spectrometer was operated under full scan from 650 to 1100 uma.

572 **Figure 5:** Partial GC-EI-MS total ion chromatograms (BPX-70 column) of (A) 4,4-dimethyloxazoline

573 (DMOX) derivatives of the isolated VLC-PC fraction obtained from bovine retina and (B) DMOX

574 derivatives of the isolated VLC-PC fraction obtained from human retina.

575 **Figure 6:** Mass spectra of 4,4-dimethyloxazoline (DMOX) derivatives of (A) 32:4n-6 and (B) 32:6n-3.

576 **Figure 7:** Concentration dependency of instrument responses. An equimolar mixture of 12 saturated

577 phosphatidylcholine (PC) species was prepared, diluted from 5 pg/µL to 5 ng/µL per species (from 60

578 pg/µL to 60 ng/µL of total PC) in chloroform/methanol (1:1) and then analyses using HPLC-ESI-MS by

579 scanning for precursors of *m/z* 184 in the positive mode. Total peak intensity versus concentration of

580 total PC.

581 **Figure 8:** Positive-ion HPLC-ESI-MS analysis of an equimolar mixture of four phosphatidylcholine

582 (PC) standards (1 ng/µL each) spiked in total lipid extract from human retina (12.5 ng/µL) by parent ion

583 scanning at −36 V collision offset. The dashed lines indicate the dependency of instrument response

584 on *m/z*. The main indicated PC species are *m/z* 678.4 = PC 28:0 (std); *m/z* 706.6 = PC 30:0, *m/z* 734

585 = PC 32:0, *m/z* 760 = PC 34:1, *m/z* 790.4 = PC 36:0 (std); *m/z* 834 = PC 40:6, *m/z* 846 = PC 44:0

586 (std); *m/z* 930 = PC 46:0 (std), *m/z* 958 = PC 48:0 (std); *m/z* 1022 = PC 54:10 and *m/z* 1050 = PC

587 56:10.

15

Figure

Figure

Figure

Figure

Figure
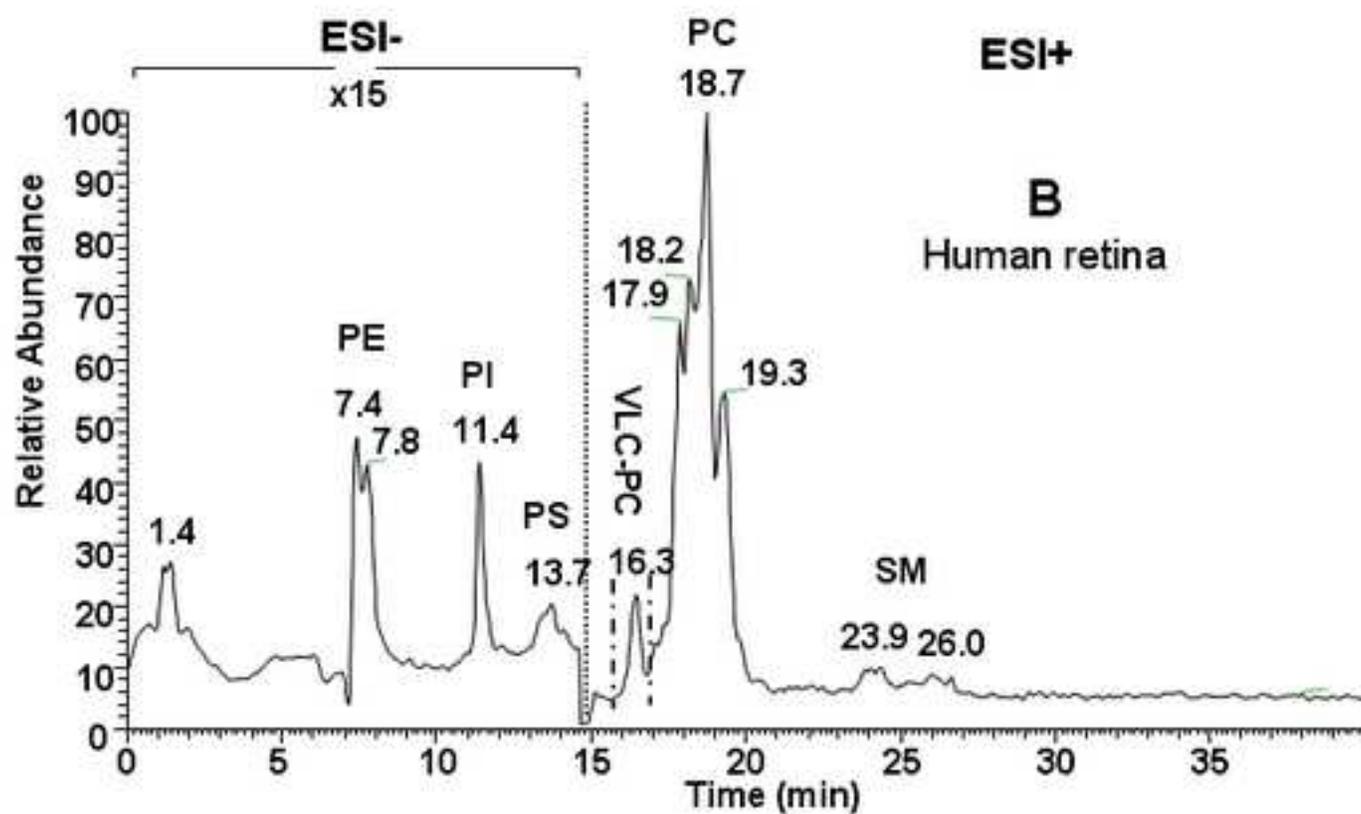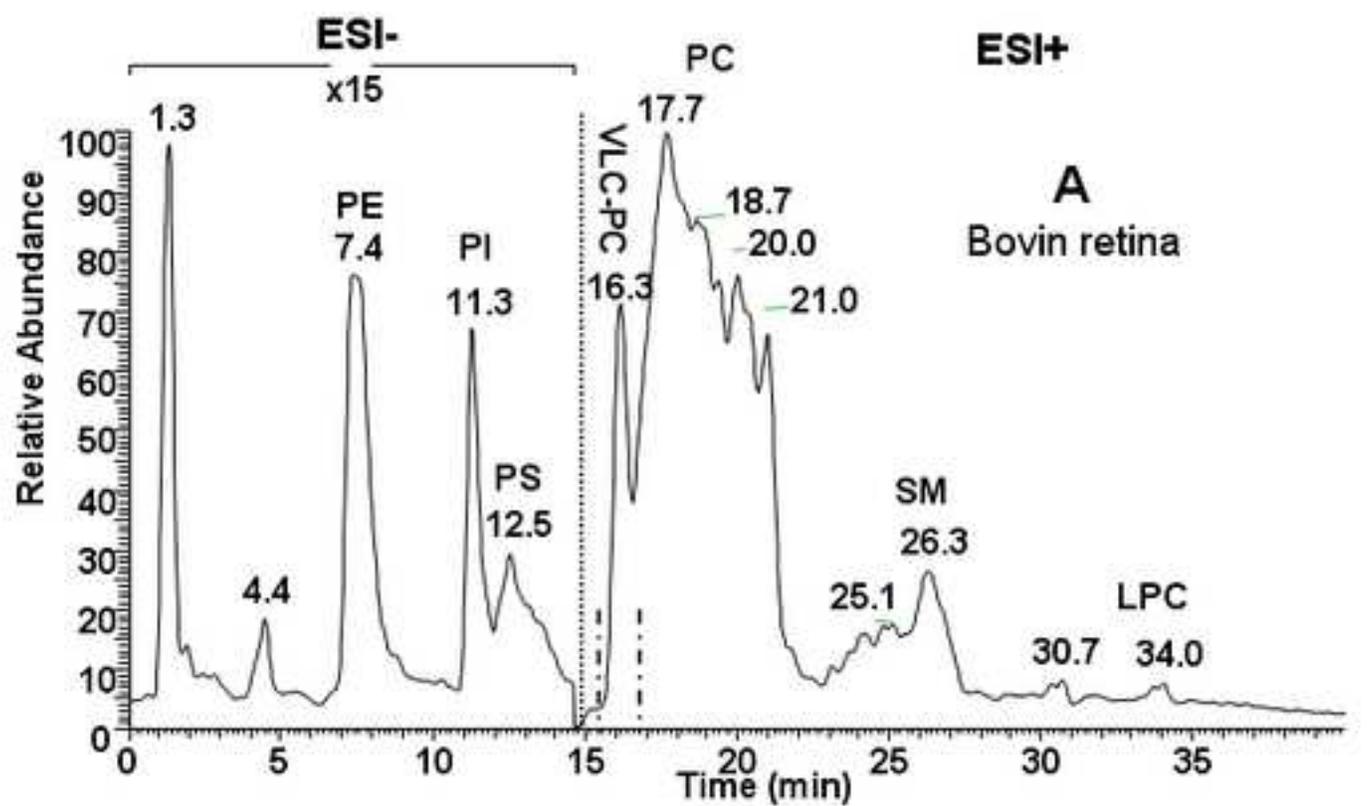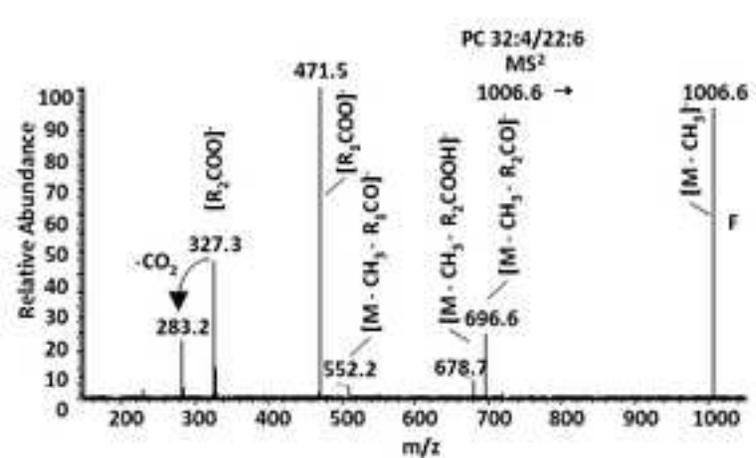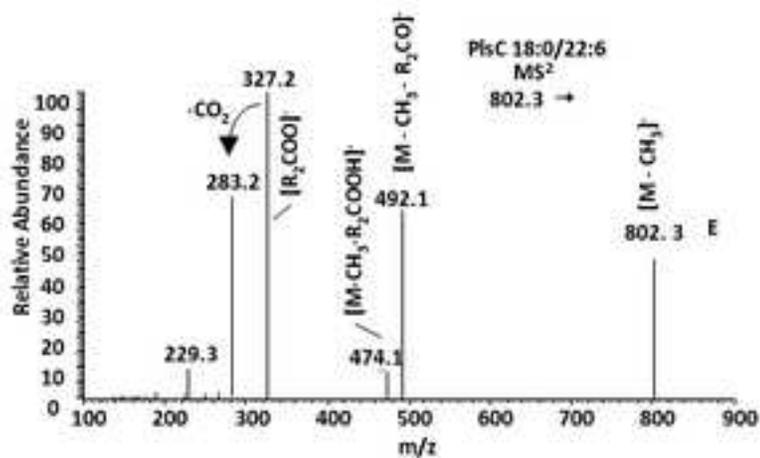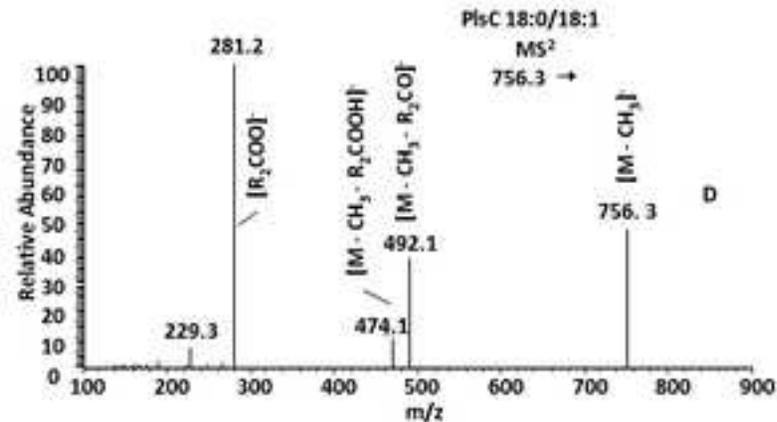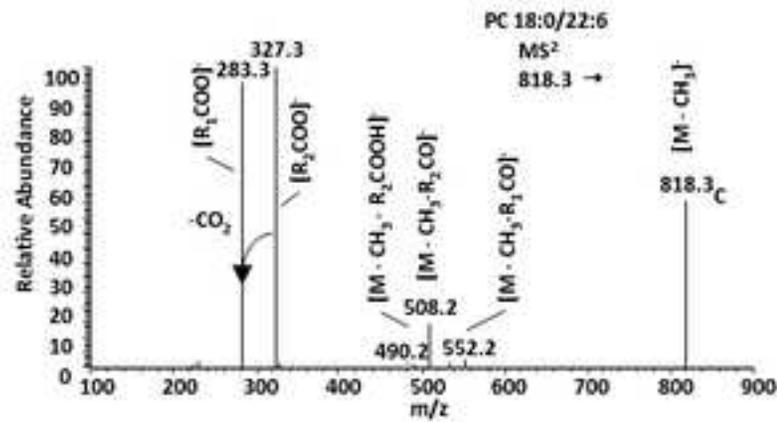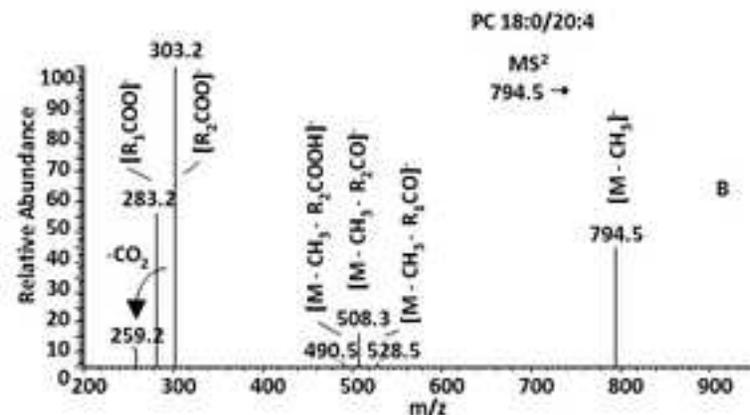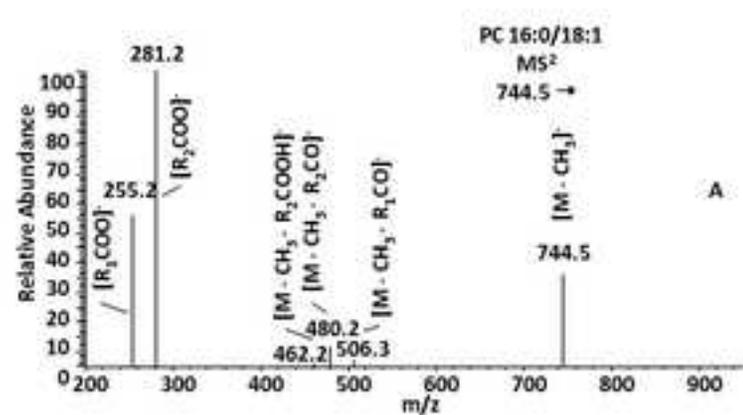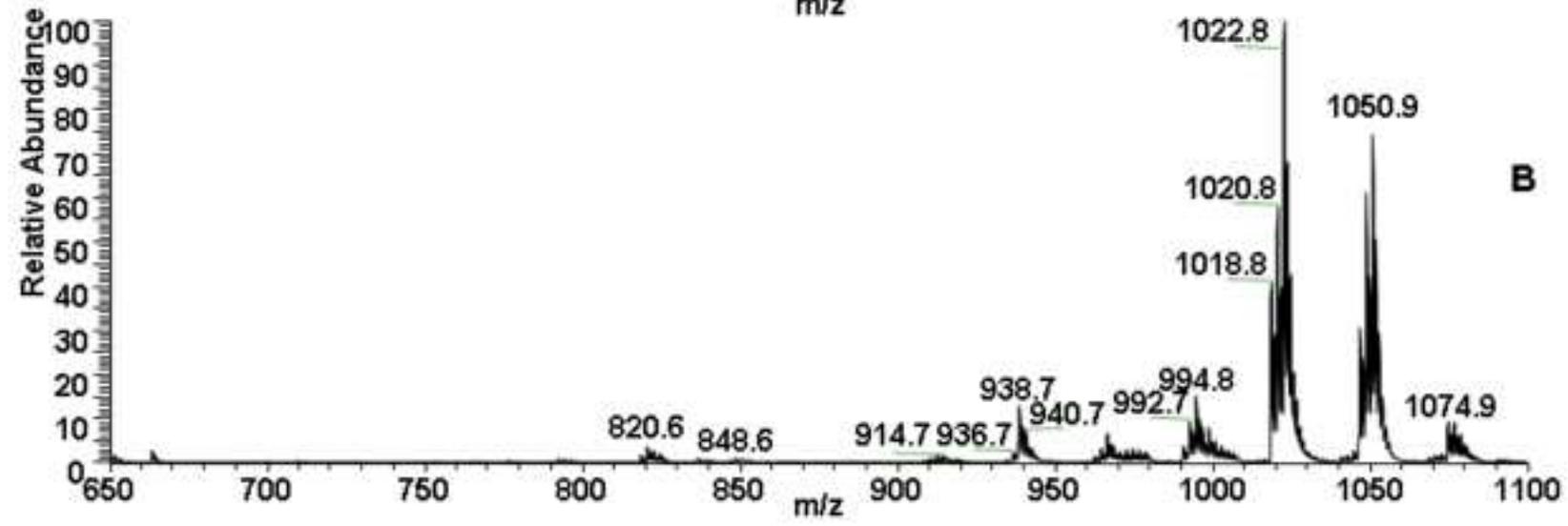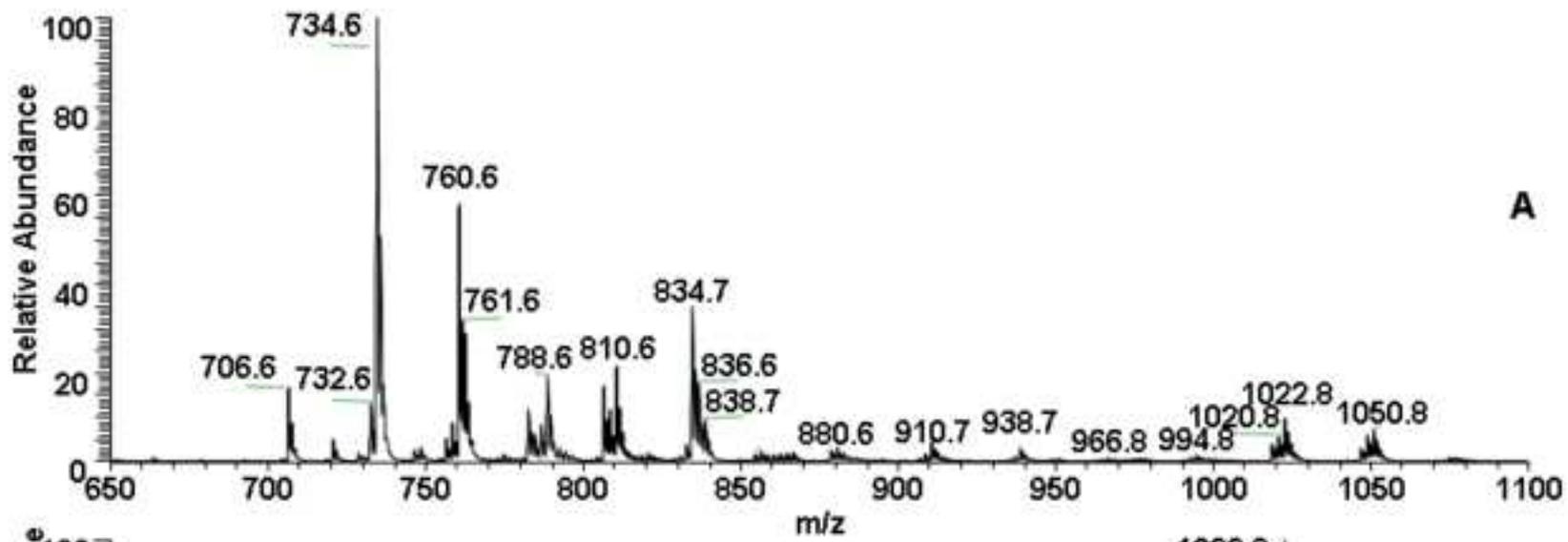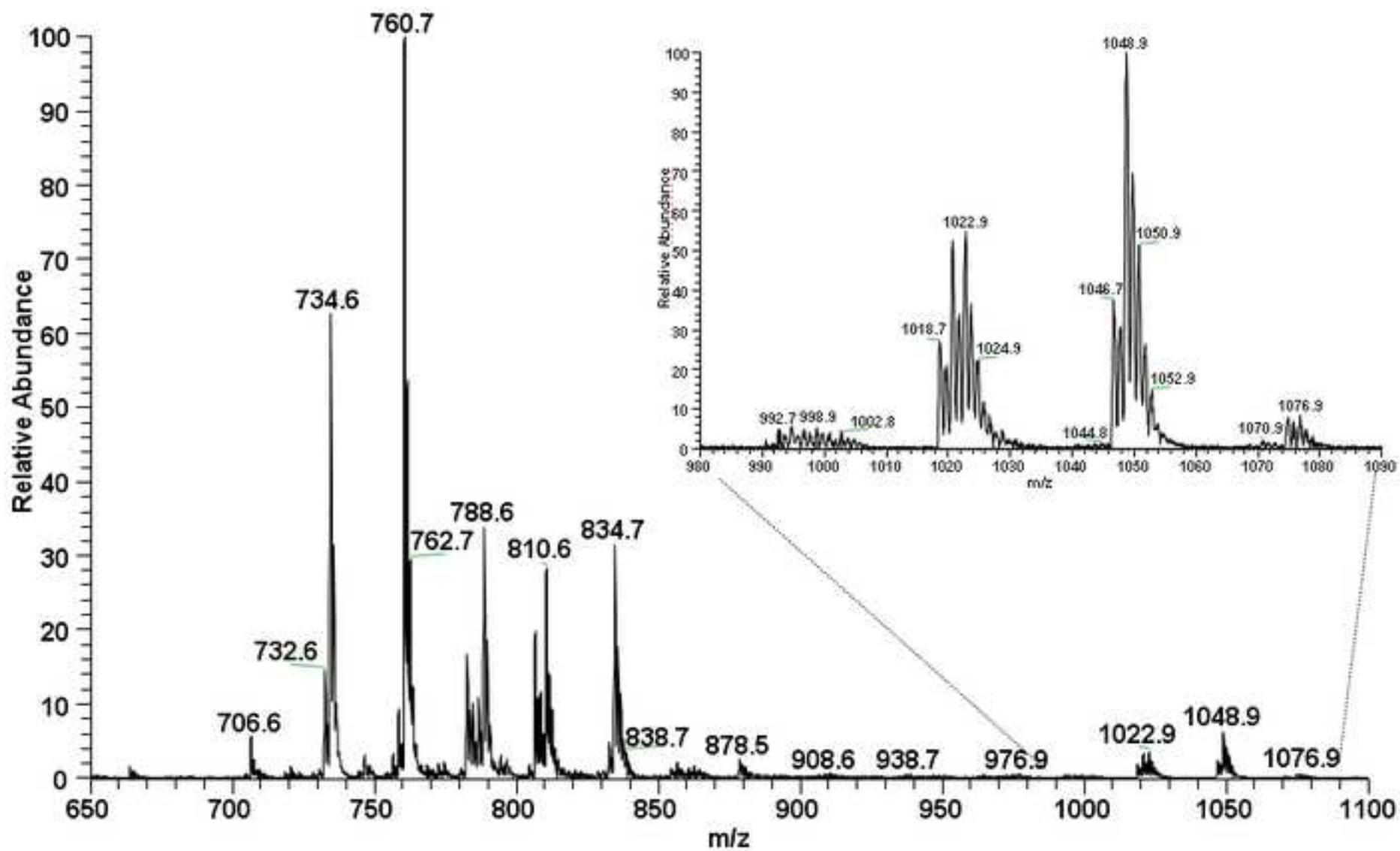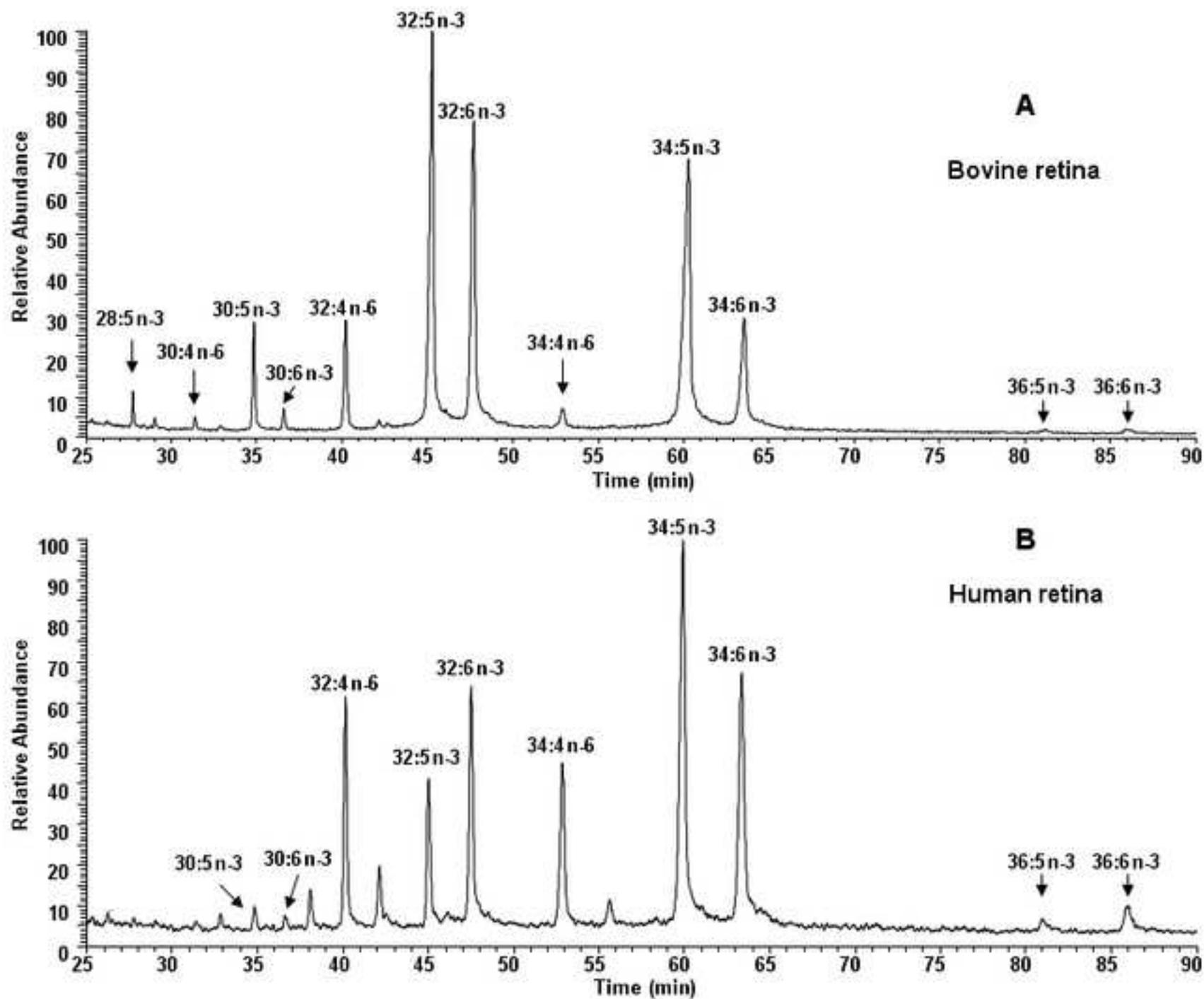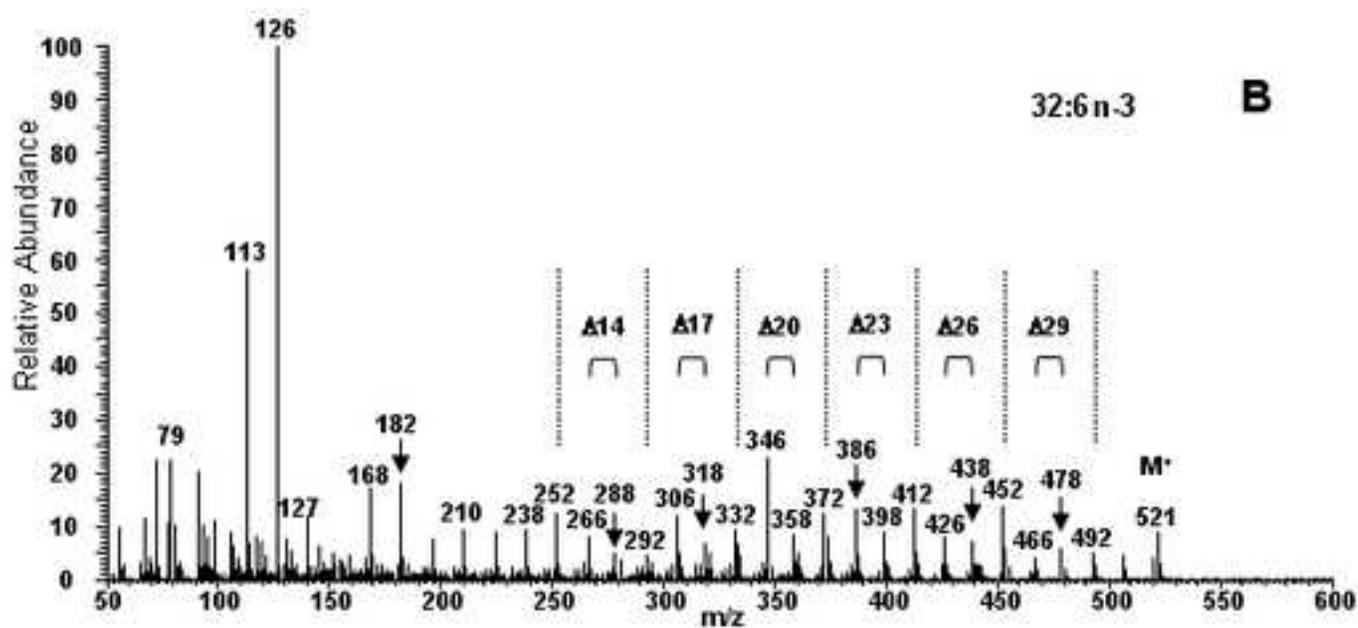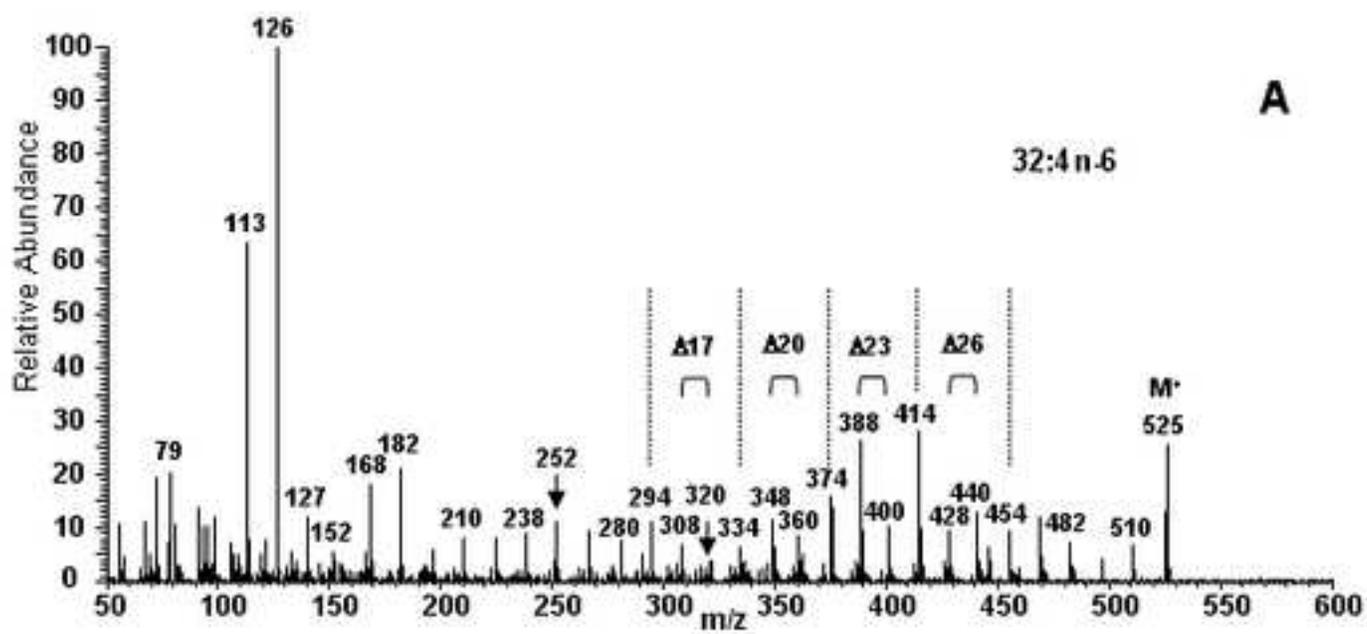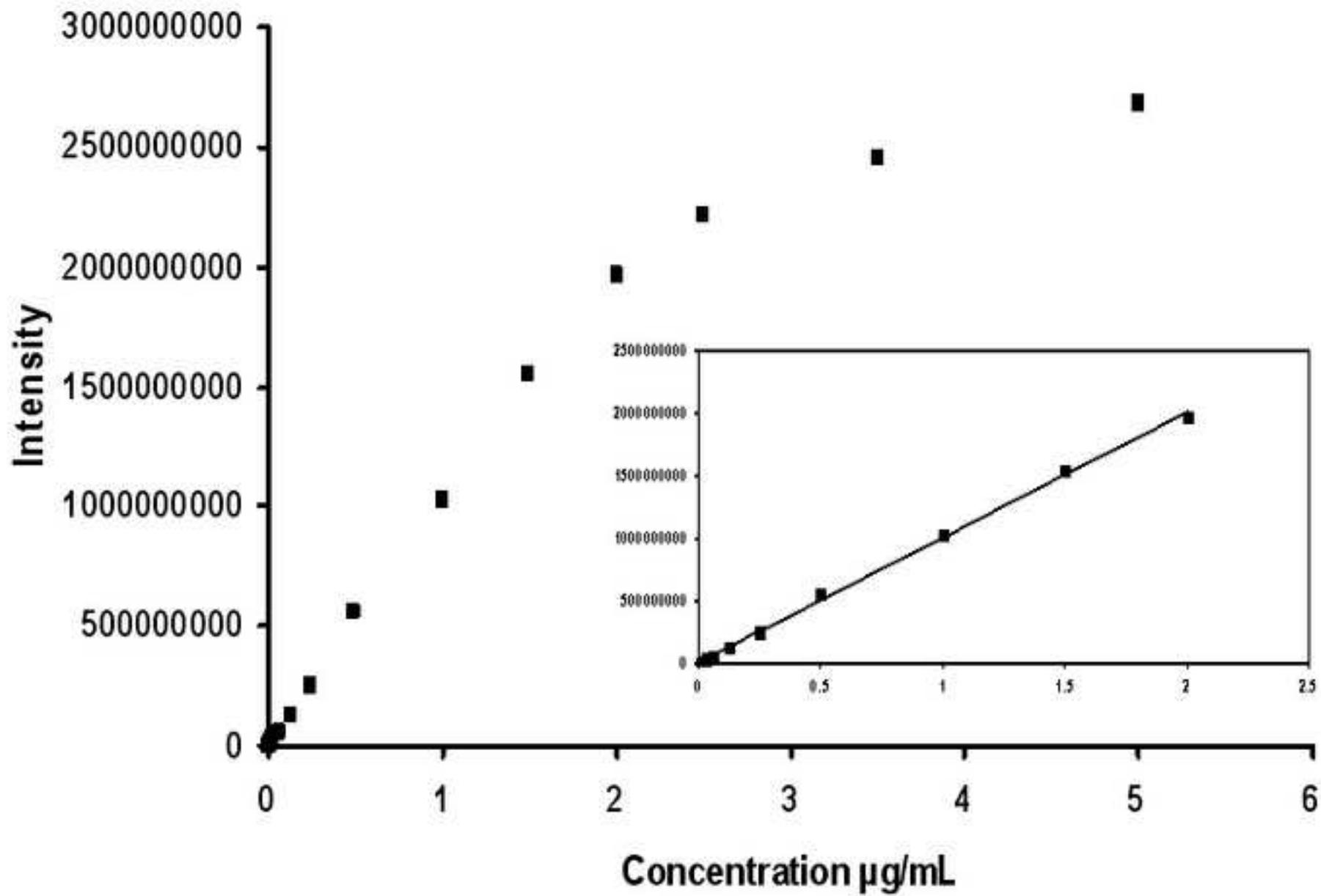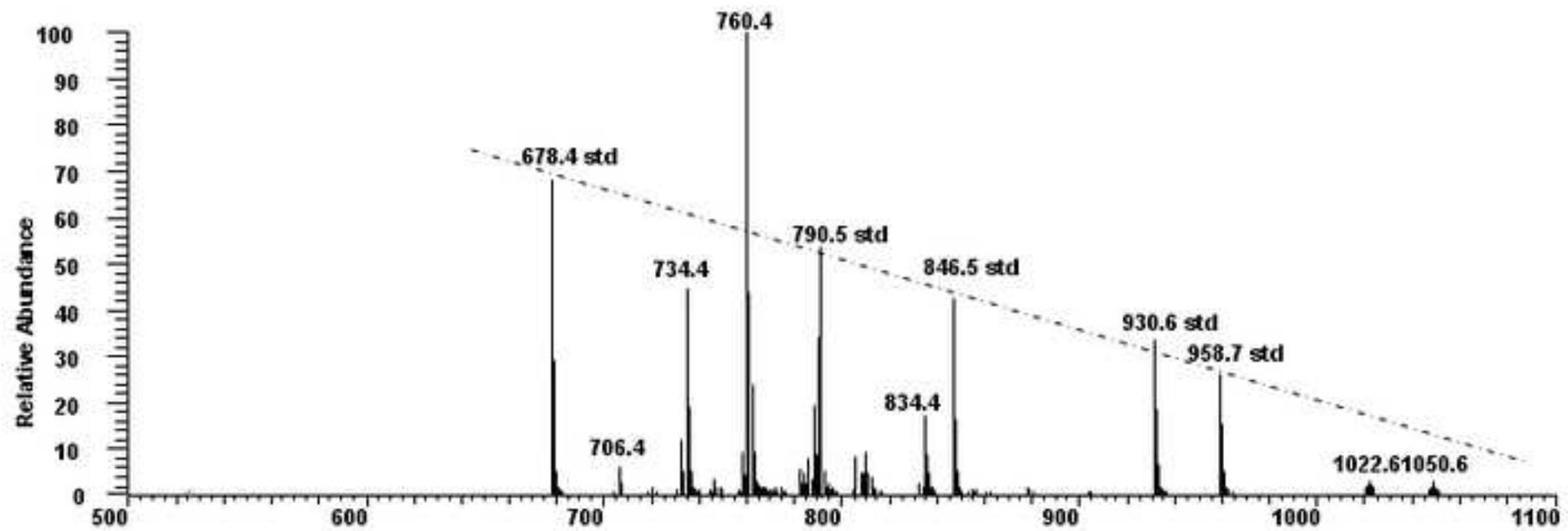
Table 1: Characterization of phosphatidylcholine molecular species in total lipid extract from bovine retina.

| Molecular species		ESI-			ESI+	Retention time (min)
		$[M-CH_3]^-$	$[R_1CH_2COO]^-$	$[R_2CH_2COO]^-$	$[M+H]^+$	
PC 30:0	PC 14:0/16:0	690.4	227.4	255.4	706.4	20.9
PlsC 32:1	PlsC p160/16:1	704.6		253.4	720.6	20.7
PC 32:2	PC 16:1/16:1	714.5	253.4	253.4	730.5	20.6
PC 32:1	PC 16:0/16:1	716.5	255.4	253.4	732.5	20.5
PC 32:0	PC 16:0/16:0*	718.5	255.4	255.4	734.6	20.0
PlsC 34:0	PlsC p180/16:0	730.5		253.4	746.5	17.2
PC 34:2	PC 16:0/18:2	742.6	255.4	279.4	758.6	18.9
PC 34:1	PC 16:0/18:1*	744.6	255.4	281.4	760.6	18.7
PC 34:0	PC 16:0/18:0	746.6	255.4	283.4	762.6	19.0
PlsC 36:0	PlsC p180/18:0	758.6		281.5	774.6	17.2
PC 36:4	PC 16:0/20:4	766.6	255.4	303.5	782.6	17.0
PC 36:3	PC 18:1/18:2	768.6	281.5	279.4	784.6	18.4
PC 36:2	PC 18:1/18:1	770.6	281.5	281.5	786.6	18.3
PC 36:2	PC 18:0/18:2	770.6	283.5	279.4	786.6	18.3
PC 36:1	PC 18:0/18:1	772.3	283.5	281.5	788.3	18.3
PC 36:0	PC 18:0/18:0*	774.7	283.4	283.5	790.7	18,3
PlsC 38:6	PlsC p160/22:6	774.7		327.5	790.7	17.2
PlsC 38:5	PlsC p181/20:4	776.7		303.5	792.7	17.1
	PlsC p160/22:5	776.7		329.5	792.7	17.1
PlsC 38:4	PlsC p180/20:4	778.7		303.5	794.7	17.0
	PlsC p160/22:4	778.7		331.5	794.7	17.0
PlsC 38:3	PlsC p180/20:3	780.7		305.5	796.7	16.9
	PlsC p18:1/20:2	780.7		308.5	796.7	16.9
PC 38:6	PC 18:2/20:4	790.5	279.4	303.5	806.6	18.0
	PC 16:0/22:6	790.5	255.4	327.5	806.6	18.0
PC 38:5	PC 18:1/20:4	792.5	281.5	303.5	808.6	17.9
	PC 16:0/22:5	792.5	255.4	329.5	808.6	17.9
PC 38:4	PC 18:0/20:4*	794.6	283.5	303.5	810.6	17.5
PC 38:3	PC 18:0/20:3	796.6	283.5	305.5	812.6	17.8
PlsC 40:6	PlsC p180/22:6*	802.6		327.5	818.6	16.9
PlsC 40:5	PlsC p181/22:4	804.6		331.5	820.6	16.8
	PlsC p180/22:5	804.6		329.5	820.6	16.6
PlsC 40:4	PlsC p180/22:4	806.6		331.5	822.7	16.6
PlsC 40:3	PlsC p181/22:2	808.6		335.5	824.7	16.5
PlsC 40:2	PlsC p181/22:1	810.5		337.6	826.6	16.5
PC 40:7	PC 18:1/22:6	816.6	281.5	327.5	832.6	17.6
PC 40:6	PC 18:0/22:6*	818.6	283.5	327.5	834.7	17.6
PC 40:5	PC 18:0/22:5	820.6	283.5	329.5	836.6	17.3
	PC 18:1/22:4	820.6	281.5	331.5	836.6	17.3
PC 40:4	PC 18:0/22:4	822.6	283.5	331.5	838.6	17.3
PC 44:12	PC 22.6/22:6	862.6	327.5	327.5	878.6	17.1
PC 44:11	PC 22.5/22:6	864.6	329.5	327.5	880.6	17.0
PC 44:10	PC 22.4/22:6	866.6	331.5	327.5	882.6	17.2
PC 44:9	PC 22:3/22:6	868.6	333.5	327.5	884.6	17.2
PC 46:12	PC 24:6/22:6	890.6	355.6	327.5	906.6	17.0
PC 46:11	PC 24.5/22:6	892.7	357.6	327.5	908.7	17.0
PC 46:10	PC 24.4/22:6	894.7	359.6	327.5	910.7	16.9
PC 46:9	PC 24:3/22:6	896.7	361.6	327.5	912.7	16.9
PC 48:12	PC 26:6/22:6*	918.7	383.7	327.5	934.7	16.9
PC 48:11	PC 26:5/22:6	920.7	385.7	327.5	936.7	16.8
PC 48:10	PC 26:4/22:6	922.7	387.5	327.5	938.7	16.8
PC 50:12	PC 28:6/22:6	946.7	411.7	327.5	962.7	16.8
PC 50:11	PC 28:5/22:6	948.7	413.7	327.5	964.7	16.6
PC 50:10	PC 28.4/22:6	950.0	415.7	327.5	966.0	16.5
PC 52:12	PC 30:6/22:6	974.7	439.7	327.5	990.7	16.5
PC 52:11	PC 30:5/22:6	976.8	441.7	327.5	992.8	16.5
PC 52:10	PC 30:4/22:6	978.8	443.7	327.5	994.8	16.4
PC 54:12	PC 32:6/22:6	1 002.7	467.7	327.5	1 018.8	16.5
PC 54:11	PC 32:5/22:6	1 004.7	469.8	327.5	1 020.8	16.3
PC 54:10	PC 32:4/22:6	1 006.8	471.8	327.5	1 022.8	16.3
PC 56:12	PC 34:6/22:6	1 030.8	495.8	327.5	1 046.8	16.2
PC 56:11	PC 34:5/22:6	1 032.8	497.8	327.5	1 048.8	16.2
PC 56:10	PC 34:4/22:6	1 034.8	499.8	327.5	1 050.8	16.1
PC 58:12	PC 36:6/22:6	1 058.8	523.9	327.5	1 074.8	16.0
PC 58:11	PC 36:5/22:6	1 060.8	525.9	327.5	1 076.9	15.9
PC 58:10	PC 36.4/22:6	1 062.8	527.9	327.5	1 078.9	15.9

* Commercial standards availables and used for identification and the calibration curves

Tables

Table 2: Characterization and quantification of phosphatidylcholine molecular species in total lipid extract from human neural retina from 9 donors.

| Molecular species | | Characterization | | | | Quantification (µg/mL) | | | | | | | | |
| | | ESI- | | | ESI+ | | | | | | | | | |
		$[M-CH_3]^-$	$[R_1CH_2COO]^-$	$[R_2CH_2COO]^-$	$[M+H]^+$	1	2	3	4	5	6	7	8	9
PC 14:0/16:0	PC 30:0	690.4	227.4	255.4	**706.4**	0.089	0.113	0.072	0.092	0.095	0.084	0.083	0.108	0.069
PlsC p160/16:1	PlsC 32:1	704.0		253.4	**720.0**	0.016	0.033	0.025	0.027	0.029	0.023	0.026	0.032	0.021
PC 16:1/16:1	PC 32:2	714.5	253.4	253.4	**730.5**	0.029	0.021	0.013	0.022	0.016	0.016	0.022	0.018	0.019
PC 16:0/16:1	PC 32:1	716.5	255.4	253.4	**732.5**	0.274	0.266	0.191	0.232	0.178	0.187	0.219	0.222	0.222
PC 16:0/16:0	PC 32:0	718.6	255.4	255.4	**734.6**	0.723	0.812	0.642	0.769	0.785	0.822	0.765	0.855	0.669
PlsC p160/18:0	PlsC 34:0	730.6		253.4	**746.6**	0.065	0.093	0.059	0.061	0.053	0.056	0.049	0.076	0.050
PC 16:0/18:2	PC 34:2	742.6	255.4	279.4	**758.6**	0.201	0.226	0.188	0.175	0.155	0.162	0.016	0.178	0.166
PC 16:0/18:1	PC 34:1	744.6	255.4	281.4	**760.6**	1.938	2.188	2.016	1.839	1.912	1.999	1.858	2.006	2.101
PC 16:0/18:0	PC 34:0	746.6	255.4	283.4	**762.6**	0.288	0.348	0.267	0.298	0.316	0.333	0.276	0.312	0.272
PC 16:0/20:4	PC 36:4	766.6	255.4	303.5	**782.6**	0.127	0.127	0.133	0.184	0.153	0.160	0.158	0.121	0.164
PC 18:1/18:2	PC 36:3	768.6	281.5	279.4	**784.6**	0.088	0.090	0.069	0.106	0.090	0.094	0.105	0.093	0.084
PC 18:1/18:1	PC 36:2	770.6	281.5	281.5	**786.6**	0.153	0.190	0.142	0.113	0.126	0.131	0.107	0.166	0.138
PC 18:0/18:1	PC 36:1	772.6	283.5	281.5	**788.6**	0.441	0.557	0.371	0.440	0.465	0.489	0.398	0.425	0.432
PC 18:2/20:4	PC 38:6	790.6	279.4	303.5	**806.6**	0.180	0.153	0.168	0.169	0.182	0.199	0.220	0.192	0.147
PC 18:1/20:4	PC 38:5	792.6	281.5	303.5	**808.6**	0.126	0.095	0.084	0.099	0.086	0.096	0.087	0.095	0.090
PC 18:0/20:4	PC 38:4	794.6	283.5	303.5	**810.6**	0.270	0.286	0.229	0.371	0.253	0.297	0.291	0.243	0.300
PC 18:0/20:3	PC 38:3	796.6	283.5	305.5	**812.6**	0.078	0.076	0.051	0.085	0.077	0.063	0.092	0.074	0.082
PlsC p181/22:6	PlsC 40:7	800.4		327.5	**816.4**	0.007	0.007	0.007	tr	0.007	0.006	0.003	0.004	0.007
PlsC p181/22:4	PlsC 40:5	804.6		331.5	**820.6**	0.011	0.009	0.006	0.010	0.007	0.008	0.008	0.008	0.008
PC 18:1/22:6	PC 40:7	816.6	281.5	327.5	**832.6**	0.056	0.043	0.044	0.043	0.051	0.052	0.045	0.053	0.044
PC 18:0/22:6	PC 40:6	818.6	283.5	327.5	**834.6**	0.467	0.314	0.327	0.456	0.397	0.425	0.532	0.425	0.404
PC 18:0/22:5	PC 40:5	820.6	283.5	329.5	**836.6**	0.092	0.059	0.060	0.112	0.088	0.085	0.107	0.077	0.083
PC 22:6/22:6	PC 44:12	862.6	327.5	327.5	**878.6**	0.048	0.015	0.013	0.008	0.011	0.025	0.017	0.044	0.013
PC 24:6/22:6	PC 46:12	890.6	355.6	327.5	**906.6**	tr	tr	tr	tr	tr	tr	tr	tr	tr
PC 24:5/22:6	PC 46:11	892.6	357.6	327.5	**908.6**	tr	tr	tr	tr	tr	0.005	tr	tr	tr
PC 24:4/22:6	PC 46:10	894.6	359.6	327.5	**910.6**	tr	tr	tr	tr	tr	tr	tr	tr	tr
PC 30:6/22:6	PC 52:12	974.7	439.7	327.5	**990.7**	tr	tr	tr	tr	tr	tr	tr	tr	tr
PC 30:5/22:6	PC 52:11	976.7	441.7	327.5	**992.7**	tr	tr	tr	tr	tr	tr	tr	tr	tr
PC 32:6/22:6	PC 54:12	1002.8	467.7	327.5	**1018.8**	0.022	0.009	0.006	0.020	0.019	0.031	0.021	0.014	0.007
PC 32:5/22:6	PC 54:11	1004.8	469.8	327.5	**1020.8**	0.022	0.009	0.006	0.020	0.019	0.031	0.021	0.014	0.007
PC 32:4/22:6	PC 54:10	1006.8	471.8	327.5	**1022.8**	0.023	0.005	0.005	0.036	0.023	0.010	0.020	0.015	0.012
PC 34:6/22:6	PC 56:12	1030.8	495.8	327.5	**1046.8**	0.030	0.010	0.018	0.024	0.024	0.016	0.038	0.028	0.023
PC 34:5/22:6	PC 56:11	1032.8	497.8	327.5	**1048.8**	0.065	0.028	0.035	0.055	0.053	0.053	0.071	0.049	0.039
PC 34:4/22:6	PC 56:10	1034.8	499.8	327.5	**1050.8**	tr	tr	tr	tr	tr	tr	tr	tr	tr
PC 36:6/22:6	PC 58:12	1058.8	523.9	327.5	**1074.8**	0.015	0.005	0.012	0.009	0.011	0.005	0.010	0.009	0.020
PC 36:5/22:6	PC 58:11	1060.9	525.9	327.5	**1076.9**	0.011	tr	0.007	0.008	tr	tr	0.007	0.004	0.011

tr < 0.005